NASA Technical Memorandum 103639

Critical-Layer Nonlinearity in the Resonance Growth of Three-Dimensional Waves in Boundary Layers

Reda R. Mankbadi
Lewis Research Center
Cleveland, Ohio

November 1990

NASA

CRITICAL-LAYER NONLINEARITY IN THE RESONANCE GROWTH OF THREE-DIMENSIONAL WAVES IN BOUNDARY LAYERS

Reda R. Mankbadi
National Aeronautics and Space Administration
Lewis Research Center
Cleveland, Ohio 44135

ABSTRACT

This paper addresses the nonlinear interactions of a triad of initially linear stability waves. The triad consisted of a single two-dimensional mode at a given frequency and two oblique modes with equal and opposite spanwise wave numbers. The oblique waves were at half the frequency and streamwise wave number of the two-dimensional mode. Attention was focused on the boundary-layer transition at low frequencies and high Reynolds numbers. A five-zoned structure and low-frequency scaling were used to derive the nonlinear-interaction equations. In this study, we analyzed the initial nonlinear development of the waves; the results indicated that the two-dimensional wave behaves according to linear theory. Nonlinear interactions caused exponential-of-an-exponential growth of the oblique modes. This resonant amplification of the subharmonic depended on the initial amplitude of the two-dimensional wave and on the initial phase angle between the two-dimensional wave and the oblique waves. The resonant growth of the oblique modes was more pronounced at lower frequencies than at higher frequencies. The results presented herein are in good agreement with experimental results and offer new explanations of the observed process.

1. INTRODUCTION

Linear stability theory indicates that, for unstable boundary layers, a Tollmein-Schlichting wave at sufficiently small amplitude would grow and, subsequently decay along the boundary layer. This, by itself, cannot explain the transition to the turbulent state and the three-dimensionality of the flow.

In the experiment of Klebanoff, Tidstrom, and Sargent (1962), a predominantly two-dimensional disturbance of prescribed frequency was introduced into the boundary layer by way of a vibrating ribbon. At relatively large Tollmein-Schlichting amplitudes, the experiment showed that a spanwise periodic three-dimensional structure evolved. This structure is characterized by spanwise alternating peaks and valleys, that is, regions of enhanced and reduced amplitude. The structure grows in intensity with downstream distance. The growth of the wave at peak positions is much larger than the original Tollmein-Schlichting growth and is in contrast to the slow Tollmein-Schlichting linear growth rate on the viscous scale.

Linear stability theory cannot account for such three-dimensional waves growing more rapidly than the two-dimensional component of the initial disturbance. To explain this discrepancy, Craik (1971), among others, proposed a resonant-triad interaction. The triad comprises a two-dimensional wave and two oblique waves propagating at equal and opposite angles to the flow direction, such that the three waves have the same phase velocity in the downstream direction. Craik's (1971) temporal stability analysis of the triad showed that the nonlinear interactions can cause a large energy transfer from the mean shear flow to the oblique waves. This energy transfer would cause the oblique waves to grow rapidly and may be responsible for the rapid development of three-dimensionality in unstable boundary layers. Craik (1971, 1978, 1985) and Usher and Craik (1975) supported this analysis by approximating the interaction coefficients for the kind of interplay that might take place. Craik accounted for the resonance in one of the experimental conditions of Klebanoff et al. (1962), but not for that observed at other conditions. Since peak-valley splitting is not associated with the subharmonic waves, however, his results were criticized.

The presence of the subharmonic of the fundamental wave at the laminar-turbulent transition in a boundary layer is now generally accepted, having been well established by such experimental observations as those of Kachanov, Koslov, and Levchenko (1977), Thomas and Saric (1981), Saric, Carter, and Reynolds (1981), Kachanov and Levchenko (1984), and Corke and Mangano (1989). The appearance of the subharmonic causes the flow to become three-dimensional. This manifests itself in the formation of λ-shaped structures arranged in staggered, alternating rows. Thus, aligned λ-structure corresponds to the peak-valley splitting, whereas the alternating one corresponds to subharmonic resonance. In the transition described by Kachanov and Levchenko (1984), the parametric resonant excitation of a pair of oblique subharmonic waves by the plane fundamental wave is the main cause of the appearance of the low-frequency fluctuation. The oscillations with the subharmonic frequency reach considerable amplitudes only in the region of the upper branch of the neutral stability curve and behind it. Kachanov and Levchenko's (1984) observations indicated that three-dimensionality can come into play initially as a resonant-triad phenomenon; this revived interest in Craik's model.

Attributing the occurrence of three-dimensionality in Klebanoff et al.'s (1962) experiment to spanwise differential amplification of Tollmein-Schlichting waves is supported by the theoretical work of Landahl (1972). However, the peak-valley splitting and the three-dimensionality of the disturbances may also be explained in the light of Craik's triad interactions by considering the two oblique waves to be at the excitation frequency but interacting with a two-dimensional wave at twice the excitation frequency. The peaks are thus given by the amplitudes of four waves: three waves at the same excitation frequency (one two-dimensional and two obliques) and a weaker two-dimensional wave at twice the frequency. The valleys are then given by the

amplitudes of two plane waves, one at the excitation frequency and one at twice the frequency. This explanation is supported by Klebanoff et al.'s (1962) and Cornelius' (1985) observation that the frequency tends to double at the valleys. With proper definition of fundamental and subharmonic frequencies, Craik's (1971) triad can apply to the transitions described by both Klebanoff et al. and Kachanov and Levenchko (1984).

Of interest here are nonlinear interactions that arise from the continued growth of a resonant triad of initially linear instability waves. The triad consists of a single two-dimensional mode at a given frequency and two oblique modes with equal and opposite spanwise wave numbers. The oblique waves are at half the frequency and the streamwise wave number of the two-dimensional mode. Attention herein is focused on the technologically significant problem of boundary-layer transition at low frequency and high Reynolds numbers. Low-frequency scaling is used to derive the nonlinear equations. In the present analysis, nonlinearity first comes into effect in the common critical layer of these modes. This is consistent with the data of Klebanoff et al. (1962), with the numerical simulations of Croswell (1985) and Singer et al. (1987), and with Craik's (1971) finding that the nonlinear energy transfer takes place mainly in the vicinity of the critical layer. The amplitude equations are obtained by equating the velocity jump calculated from outside the critical layer to the velocity jump calculated from the solution within the critical layer.

Two regimes of fundamental-subharmonic interactions can be identified in Kachanov and Levchenko's (1984) experiment. In the initial development of the three-dimensionality, the subharmonic is smaller than the fundamental, and the latter behaves as if the former is not present. Thus, although the subharmonic resonates, the fundamental is still given by its linear growth rate. In a second stage, where the subharmonic exceeds the fundamental, a back-reaction

process is observed in which the two waves behave nonlinearly. The initially negligible back-reaction on the two-dimensional wave allows the oblique modes to exhibit faster-than-exponential growth, while the two-dimensional mode continues to grow at its initial linear growth rate. This initial nonlinear interaction of the waves is the subject of the present study.

The overall plan of this paper is as follows: the five-zoned structure and the scaling are discussed in section 2; the linear solution is obtained in section 3 (the nonlinear critical-layer interaction gradually evolves from a resonant triad of strictly linear, small growth rate and low-frequency solutions); in section 4, the critical-layer flow is considered; then, the amplitude equations are obtained in section 5, where the relevant expansions are worked out, and the solution that matches the solution outside the critical layer is then found by taking the Fourier transforms with respect to the cross-stream coordinate (the resulting solution is restricted to the case where the order of the oblique waves is not much larger than that of the two-dimensional wave); the solution of the amplitude equations in the nonlinear region is presented in section 6; the composite solution that matches the upstream linear solution is formed in section 7 (this leads to a different type of amplitude equation that involves upstream history effects and is different from that of Craik (1971)); results and discussions are presented in section 8; and a detailed comparison to available data is given in section 9. The experimental comparisons seem very encouraging, yielding both qualitative and quantitative agreement. The results presented herein explain the observed subharmonic resonance and the three-dimensionality of the flow. New features of the subharmonic resonance are discussed.

2. FIVE-ZONED STRUCTURE AND SCALING

The upstream flow starts as a resonant triad (fig. 1) of linear, spatially growing instability waves: a single two-dimensional mode of normalized frequency ω and wave number α; and two subharmonic oblique modes of frequency $\omega/2$, streamwise wave number nearly equal to $\alpha/2$, and spanwise wave number $\pm\beta$. All velocities are normalized by the upstream velocity U_∞, lengths by δ^*, time by δ^*/U_∞, and pressure by ρU_∞^2, where ρ is the fluid density and δ^* is the boundary-layer thickness defined as $\delta^* = \sqrt{\nu x/U_\infty}$.

The flow under consideration here is that of a laminar boundary layer of Blasius profile (fig. 2). The development of the waves outside the nonlinear region follows the weakly nonparallel linear theory. In the nonlinear region, the unsteady flow is not affected by the boundary layer growth over the region in which the nonlinear interaction takes place. The experimental observations of Kachanov and Levchenko (1984), Saric et al. (1984), and Corke and Mangano (1987, 1989) have indicated that subharmonic resonance takes place in the vicinity and beyond the upper branch of the neutral stability curve. Goldstein and Durbin (1986) showed that upper-branch scaling applies over almost all of the unstable region, only breaking upstream in the close proximity of the lower branch. In this range of Reynolds number, the disturbance solution is a five-zoned structure (see Drazin and Reid 1981, Graebel 1966, Eagles 1969, Fraenkel 1969, DeVillers 1975), as shown in figure 3. Zone I is the closest to the wall, where the unsteady viscous sublayer reduces to zero the effect of the streamline displacement at the wall. Zone II is an inviscid rotational zone of adjustment within which the critical layer III is induced. Zone IV is above zone II; it is an inviscid rotational region comprising most of the boundary layer, and it is the place where the disturbance nearly provokes a small quasi-steady displacement of the streamlines of the basic boundary-layer

flow. Above zone IV, the displacement also provokes the quasi-steady zone V, lying outside the boundary layer, in which the flow properties are of an inviscid irrotational type because the basic flow is almost the free stream $U = 1$, $V = 0$, where U is the velocity component in the flow direction and V is the perpendicular component in the y-direction.

The normalized complex wave number α is small, and its imaginary part is smaller than its real part (Reid, 1965; and Goldstein, Durbin, and Leib, 1987). Then each of the three modes has a critical layer at nearly the same transverse position y_c, where the real part of their nearly common phase velocity c is equal to the streamwise velocity U.

The mean boundary-layer velocity is given by the Blasius velocity U_B, where

$$U_B = \lambda y - \frac{\lambda^2}{2 \cdot 4!} y^4 + \ldots , \qquad \text{as} \qquad y \to 0 . \tag{2.1}$$

The wall is located at $y = 0$, and the constant λ denotes the scaled Blasius skin friction ($\lambda = 0.332$ in the present coordinates).

We introduce the asymptotically small parameter σ, where

$$\bar{R} = \sigma^{10} R . \tag{2.2a}$$

This small parameter σ can be related to the normalized frequency F^*, as in Goldstein and Durbin (1986), by

$$F^* \equiv \frac{\omega \nu}{U_\infty^2} = \sigma^{12} . \tag{2.2b}$$

Here, R is the Reynolds number based on the local momentum thickness, $\bar{R}$ is an order-one scaled Reynolds number and is a real quantity for time-periodic, spatially growing disturbances, and

$$\bar{c} = \frac{\bar{R}}{\bar{\alpha}} \tag{2.3}$$

where $\bar{c}$ and $\bar{\alpha}$ are order-one real constants. Goldstein et al. (1987) showed that the most rapidly growing modes correspond to the scaling

$$Re\ \alpha = \sigma\bar{\alpha} + O(\sigma^4) , \tag{2.4}$$

$$Re\ c_o = \sigma\bar{c}_o + O(\sigma^4) , \tag{2.5}$$

$$\beta = \sigma\bar{\beta} , \tag{2.6}$$

and

$$y_c = \sigma Y_c + O(\sigma^4) , \tag{2.7}$$

where $\bar{\beta}$ is an order-one real spanwise wave number, Y_c is an order-one real constant, and c_o is the phase velocity of the two-dimensional wave. The scaling of α and R given by equations (2.4) and (2.2a) is consistent with Reid's (1965) equation (3.128).

3. LINEAR SOLUTION

Outside the critical layer the unsteady flow is governed by the linear dynamics, as first pointed out by Haberman (1972), and the velocity field is given by

$$u = U_B(y) + Re\left\{\varepsilon A_o(x_1)\frac{\partial \Phi_o}{\partial y}(y,x_1,\sigma)e^{iX} + \delta A(x_1)\left[U_+(y,x_1,\sigma)e^{iZ} + U_-(y,x_1,\sigma)e^{-iZ}\right]e^{iX/2}\right\} , \tag{3.1}$$

$$v \equiv Re\ i\left[\varepsilon\alpha A_o\Phi_o e^{iX} + \delta\gamma A(e^{iZ} + e^{-iZ})\Phi e^{iX/2}\right] , \tag{3.2}$$

and

$$w = \delta\ Re\ A\left(W_+e^{iZ} + W_-e^{-iZ}\right)e^{iX/2} , \tag{3.3}$$

where

$$x_1 \equiv \sigma^4 x , \tag{3.4}$$

$$X \equiv \sigma\bar{\alpha}(x - \sigma\bar{c}t) \ , \tag{3.5}$$

$$Z \equiv \sigma\bar{\beta}z \ , \tag{3.6}$$

and

$$\bar{\gamma} \equiv \sqrt{\left(\frac{\bar{\alpha}}{2}\right)^2 + (\bar{\beta})^2} \ . \tag{3.7}$$

The amplitudes A_0 and A are for the two-dimensional and the oblique waves, respectively. The symbols ε and δ are the measure of the amplitudes of the two-dimensional and the oblique instability waves, respectively. Since the initial development of the instability waves is linear, we can take $A(x_1)$ to initially be a real quantity, but we allow the two-dimensional amplitude $A_0(x_1)$ to be complex. Later on, because of the nonlinear effects, both $A(x_1)$ and $A_0(x_1)$ become complex. In equations (3.1) and (3.2), $U_\pm$ and $W_\pm$ are related to Φ through the relations

$$\frac{\sqrt{\gamma^2 - \beta^2}}{\gamma} U_\pm \pm \frac{\beta}{\gamma} W_\pm = D\Phi \ , \tag{3.8}$$

$$\frac{\beta}{\gamma} U_\pm \mp \frac{\sqrt{\gamma^2 - \beta^2}}{\gamma} W_\pm = \frac{\beta U'}{\sqrt{\gamma^2 - \beta^2}} \left(\frac{\Phi}{U - c}\right) \tag{3.9}$$

and

$$D = \frac{\partial}{\partial y} \ . \tag{3.10}$$

By using the Squire (1933) transformation, the linearized equations for Φ_0 and Φ are

$$\left(D^2 - \alpha^2\right)^2 \Phi_0 = i\alpha R\left[(U - c_0)(D^2 - \alpha^2)\Phi_0 - U''\Phi_0\right] \tag{3.11}$$

and

$$\left(D^2 - \gamma^2\right)^2 \Phi = i\gamma R\left[(U - c)(D^2 - \gamma^2)\Phi - U''\Phi\right] , \tag{3.12}$$

where the primes denote differentiation with respect to the relevant arguments. The solutions of equations (3.11) and (3.12) are subject to the wall boundary conditions

$$\Phi = \Phi_0 = 0 \quad \text{at} \quad y = 0 \tag{3.13}$$

and

$$\Phi' = \Phi_0' = 0 \quad \text{at} \quad y = 0 \tag{3.14}$$

The complex wave numbers α and γ and the phase velocities c_0 and c are given by

$$\alpha = \sigma\bar{\alpha} + \sigma^4 \frac{A_0'}{iA_0} , \tag{3.15}$$

$$\gamma = \sigma\bar{\gamma} + \frac{\sigma^4}{2i} \frac{\bar{\alpha}}{\bar{\gamma}} \frac{A'}{A} , \tag{3.16}$$

$$c_0 = \frac{\sigma\bar{c}}{1 + \dfrac{\sigma^3}{i\bar{\alpha}} \dfrac{A_0'}{A_0}} , \tag{3.17}$$

and

$$c = \frac{\sigma\bar{c}}{1 + 2\dfrac{\sigma^3}{i\bar{\alpha}} \dfrac{A'}{A}} . \tag{3.18}$$

Equations (3.8) and (3.9) can be manipulated to produce

$$U_{\pm}\cos\theta \pm W_{\pm}\sin\theta = D\Phi - \frac{2\sigma^3}{\bar{\alpha}} \frac{U'}{U - c} \Phi \frac{A'}{iA} \sin^2\theta , \tag{3.19}$$

where

$$\theta = \sin^{-1} \frac{\bar{\beta}}{\bar{\gamma}} \tag{3.20}$$

is the propagation angle of the oblique waves.

3.1. Solution in Viscous Sublayer (Zone I)

For the viscous effects to come into play in this region, the scaling for y should be

$$y = \sigma^4 \hat{y} \ , \tag{3.1.1}$$

where $\hat{y}$ is order one. In the classical theory, the wall layer thickness is order $(\alpha Rc)^{-1/3}$ which is order $O(\sigma^4)$, consistent with equation (3.1.1). Substituting (2.1) into (3.11) and (3.12), we obtain, up to the required order of approximation,

$$\left[\hat{D}^4 - i\hat{\alpha}\bar{R}(\lambda\sigma^3\hat{y} - \hat{c})\hat{D}^2\right]\hat{\Phi} = 0 \ , \tag{3.1.2}$$

where $\hat{\Phi}$ represents Φ_0 or Φ; $\hat{\alpha}$ represents $\bar{\alpha}$ or $\bar{\gamma}$; $\hat{c}$ represents $\bar{c}_0$ or $\bar{c}$; and $\hat{D}$ is the derivative with respect to $\hat{y}$. We expand $\hat{\Phi}$ as

$$\hat{\Phi} = g_0 + \sigma g_1 + \sigma^2 g_2 + \sigma^3 g_3 + \ldots \ , \tag{3.1.3}$$

and with $\hat{\alpha}$ and $\hat{c}$ expanded according to (3.15) to (3.18), we obtain

$$\left(\hat{D}^4 + i\bar{R}\hat{\alpha}\,\hat{c}_0\hat{D}^2\right)g_0 = 0 \ . \tag{3.1.4}$$

The solution of (3.1.4) not only must decay as $\hat{y} \to \infty$ but it also is subject to the conditions

$$g_0(0) = g_0'(0) = 0 \ . \tag{3.1.5}$$

The first-order solution is given by

$$g_0 = \frac{b_0}{m}\left(m\hat{y} - 1 + e^{-m\hat{y}}\right) \ , \tag{3.1.6}$$

$$m^2 = -i\bar{\alpha}\bar{R}c_0 \ , \tag{3.1.7}$$

where b_0 is an arbitrary constant to be determined by matching with the solution at zone II. A similar solution is obtained for the oblique waves.

The corresponding velocity components are given by

$$u = Re\left[\varepsilon A_o b_o\left(1 - e^{-m\hat{y}}\right)e^{iX} + \delta Ab \cos\theta\ 2\cos Z\left(1 - e^{-M\hat{y}}\right)e^{iX/2} + \ldots\right] , \tag{3.1.8}$$

$$v = Re\left[-i\sigma^5 \bar{\alpha}\frac{b_o}{m}\left(m\hat{y} + e^{-m\hat{y}} - 1\right)\varepsilon A_o e^{iX}\right.$$

$$\left. - i\sigma^5 \bar{\gamma}\frac{b}{M}\left(M\hat{y} + e^{-M\hat{y}} - 1\right)\delta A\ 2\cos Z\ e^{iX/2} + \ldots\right] , \tag{3.1.9}$$

and

$$w = Re\left[2ib \sin Z \sin\theta\left(1 - Me^{-M\hat{y}}\right)\delta A e^{iX/2} + \ldots\right] , \tag{3.1.10}$$

where

$$M^2 = -\bar{i}\bar{\gamma}\bar{R}c . \tag{3.1.11}$$

3.2. The Tollmein Region (Zone II)

As pointed out by Goldstein, Durbin, and Leib (1987), the solution for this region is obtained by introducing the scaled transverse coordinate

$$Y = \frac{y}{\sigma} \tag{3.2.1}$$

directly into equations (3.11) and (3.12) and by using equations (2.1) and (3.15) to (3.18). The solution is obtained in the form

$$\hat{\Phi} = \sigma\left[\left(c_1 + \sigma c_2 + \sigma^2 c_3\right) + \left(c_2 + \sigma c_4 + \sigma^2 c_6\right)Y\right] + \sigma^4 F . \tag{3.2.2}$$

As will be shown, the matching requirements give $c_1 = c_2 = c_3 = 0$; therefore, the solution can be written as

$$\hat{\Phi} = \sigma(\lambda + \sigma a)Y + \sigma^4 F(Y,\phi) \tag{3.2.3}$$

where a is an order-one constant that depends on σ, and F satisfies the relation

$$\frac{\partial^2 F}{\partial Y^2} = \mu_c\left(1 + \frac{Y_c}{Y - Y_c}\right) - \frac{1}{4}\lambda^2 Y(Y_c + Y) \ , \qquad (3.2.4)$$

where

$$\mu_c = -\frac{\lambda^2 Y_c^2}{4} \qquad (3.2.5)$$

and $\bar{c} = \lambda Y_c$.

Since equation (3.2.4) is singular at $Y = Y_c$, F can be discontinuous across Y_c, and $F^{\pm}$ denotes the solution above or under this point. Integrating equation (3.2.4) gives

$$F^{\pm}(Y,\phi) = F(0) + \mu_c\left\{\frac{1}{2}Y^2 + Y_c\left[(Y - Y_c)\left(\ln|Y - Y_c| + i\hat{\phi}^{\pm}\right) + Y_c\left(\ln Y_c + i\hat{\phi}^{-}\right)\right]\right\} - \frac{\lambda^2}{4\cdot 3!}Y^3\left(Y_c + \frac{1}{2}Y\right) \ , \qquad (3.2.6)$$

where the normal velocity is continuous across the critical layer. The constants of integration $\phi^{\pm}$ and $\phi_0^{\pm}$ are, in general, a complex function of x_1. The value of F as $Y \to 0$ is $F(0)$, which is determined via matching with the solution in zone I. The corresponding velocity components are given by

$$u = Re\ \varepsilon A_0\left[(\lambda + \sigma a) + \sigma^3 F(Y,\phi)\right]e^{iX} + 2\delta A \cos Z\left[(\lambda + \sigma a)\cos\theta + \frac{U'}{U - c} \times \sin\theta \tan\theta\, \sigma(\lambda + \sigma a)Y + \sigma^3 \cos\theta\, F'(Y,\phi) + \sigma^4 \frac{U'}{U - c}\sin\theta \tan\theta\, F(Y,\phi)\right]e^{iX/2} \ , \qquad (3.2.7)$$

$$v = Re\ \left\{-\varepsilon A_0 i\bar{\alpha}\sigma^2\left[(\lambda + \sigma a_0)Y + \sigma^3 F(Y,\phi)\right]e^{iX} - \delta A i\bar{\gamma}\sigma^2\left[(\lambda + \sigma a)Y + \sigma^3 F(Y,\phi)\right]2\cos Z\, e^{iX/2}\right\} , \qquad (3.2.8)$$

and

$$w = Re\left\{2i\ \delta A \sin Z \sin\theta\left[(\lambda + \sigma a) - \frac{U'}{U - c}\,\sigma(\lambda + \sigma a)Y + \sigma^3 F(Y,\phi) - \frac{U'}{U - c}\,\sigma^4 F(Y,\phi)\right]e^{iX/2}\right\}. \qquad (3.2.9)$$

3.3. Solution in Zones IV and V

Miles' (1962) solution, which is uniformly valid for $y = O(1)$ and $y \gg 1$ in the limit as $\gamma,\alpha \to 0$, is given by

$$\frac{D\Phi}{\Phi} = \frac{U'}{U - \hat{c}} - \frac{1}{(U - \hat{c})^2\Omega^*} + O(\hat{\alpha}^5) \qquad (3.3.1)$$

where

$$\Omega^* = \frac{1}{\hat{\alpha}(1 - \hat{c})^2} + \Omega_o + \hat{\alpha}\Omega_1 + \hat{\alpha}^2\Omega_2 + \ldots , \qquad (3.3.2)$$

$$\Omega_o = -\frac{1}{(1 - \hat{c})^2}\int_y^\infty \left[\frac{(U - \hat{c})^2}{(1 - \hat{c})^2} - \frac{(1 - \hat{c})^2}{(U - \hat{c})^2}\right]dy , \qquad (3.3.3)$$

$$\Omega_1 = -\frac{2}{(1 - \hat{c})^2}\int_y^\infty (U - \hat{c})^2\Omega_o dy , \qquad (3.3.4)$$

and

$$\Omega_2 = -\int_y^\infty (U - \hat{c})^2\left[\frac{2\Omega_1}{(1 - \hat{c})^2} + \Omega_o^2\right]dy . \qquad (3.3.5)$$

By substituting equations (3.3.1) to (3.3.4) into the classical "inviscid function" (Lin, 1955, p. 37), which is defined as

$$W \equiv \frac{\hat{c}D\hat{\Phi}}{U'\hat{\Phi} - (U - \hat{c})D\hat{\Phi}} , \qquad (3.3.6)$$

and by inserting $U = U_B$ and equations (3.15) to (3.18) into the result, expanding for small σ, and then using equation (2.1), we obtain

$$W = W^{\dagger}(y;\sigma,\bar{c},\bar{\gamma}) + \sigma^3 \frac{i\bar{c}\lambda}{\bar{\gamma}^2}\left(\cos\theta + \frac{1}{\cos\theta}\right)\frac{A'}{A} \tag{3.3.7}$$

and

$$W_o = W^{\dagger}(y;\sigma,\bar{c}_o,\bar{\alpha}) + \sigma^3 \frac{2i\bar{c}\lambda}{\bar{\alpha}^2}\frac{A'_o}{A_o} , \tag{3.3.8}$$

where

$$W^{\dagger}(y;\sigma,\bar{c},\hat{\alpha}) = \frac{U'\bar{c}}{\hat{\alpha}}(1-\sigma\bar{c})^{-2} - \frac{\sigma\bar{c}\lambda}{(1-\sigma\bar{c})^4}\left[J_1 + 2\sigma\bar{c}J_2 + \sigma^2\bar{c}^2J_3 + \frac{1}{8\lambda}y^2 + O(y^3)\right]$$

$$+ \sigma^2\hat{\alpha}\bar{c}\lambda\left[J_4 + \sigma\bar{c}J_5 - \frac{1}{4\lambda^3}y + O(y^2)\right] + \sigma^3\bar{c}\left[\frac{\bar{\mu}_c}{\lambda^2}\ln y - \frac{7}{48}\frac{\bar{c}^2}{\lambda^2} + O(y)\right] . \tag{3.3.9}$$

Coefficients J_1 to J_5 are defined in the appendix.

3.4. Matching Solutions

Matching the solution in zone I and the solution in zone II is easily done by matching the velocities. The inner solution for the two-dimensional wave (eqs. (3.1.8) to (3.1.10)) as $\hat{y} \to \infty$, reduces to

$$u = Re\ b_o e^{iX} , \tag{3.4.1}$$

$$v = Re\left[-i\alpha\sigma^5 b_o\left(\hat{y} - \frac{1}{m}\right) + \ldots\right]e^{iX} . \tag{3.4.2}$$

For the solution in zone II (eqs. (3.2.7) to (3.2.9)), as $Y \to 0$, we have

$$u = Re\left[\lambda + \sigma a + \sigma^3 F'(0) + \ldots\right]e^{iX} , \tag{3.4.3}$$

$$v = Re\left[-i\sigma^5\bar{\alpha}_o F'(0) + \ldots\right]e^{iX} . \tag{3.4.4}$$

Matching the u-velocities gives

$$b_o = \lambda , \tag{3.4.5}$$

whereas matching the v-velocities gives the imaginary part of $F(0)$ as

$$F_i(0) = \frac{-\lambda}{\sqrt{2\bar{c}_o\bar{R}\bar{\alpha}}} . \tag{3.4.6}$$

Matching the velocities of the obliques waves produces similar expressions, with $\bar{c}$ replacing $\bar{c}_0$ and $\bar{\gamma}$ replacing $\bar{\alpha}$.

Matching the solution in zone II and the outer solution in zones IV and V is most easily achieved by using the inviscid function. The inviscid function for the solution in zone II is obtained by substituting equation (3.2.3) into equation (3.3.6) and re-expanding:

$$\hat{W} = \frac{U}{\lambda} + \sigma^3\left[\frac{\mu_c Y_c}{\lambda}\left(\ln\frac{Y - Y_c}{Y_c} - i\Delta\hat{\phi}\right) - \frac{F(0)}{\lambda Y_c} - \frac{1}{8}\lambda Y_c Y(2Y_c + Y)\right] + O(\sigma^4) \qquad (3.4.7)$$

for $Y > Y_c$, where $\Delta\hat{\phi}$ denotes either $\left(\phi^- - \phi^+\right)$ or $\left(\phi_0^- - \phi_0^+\right)$. Matching equations (3.3.7) and (3.3.8) shows that

$$\bar{\gamma} = \bar{\alpha} + \sigma^3 2\,\mathcal{I}m\frac{A_0'}{A_0} + O(\sigma^4)\ , \qquad (3.4.8)$$

$$\lambda\frac{\bar{c}}{\bar{\alpha}}(1 - \sigma\bar{c})^{-2} - 1 - \frac{\sigma\bar{c}\lambda}{(1 - \sigma\bar{c})^4}\left(J_1 + 2\sigma\bar{c}J_2 + \sigma^2\bar{c}^2J_3\right) + \sigma^2\bar{\alpha}\bar{c}\lambda\left(J_4 + \sigma\bar{c}J_5\right)$$

$$+ \sigma^3\left[\bar{c}\left(\frac{\bar{\mu}_c}{\lambda}\ln Y_c - \frac{7}{48}\frac{\bar{c}^2}{\lambda^2} - \frac{2\lambda}{\bar{\alpha}^2}\,\mathcal{I}m\frac{A_0'}{A_0}\right) - \frac{F_r(0)}{\lambda Y_c} + \frac{\lambda Y_c^3}{4\lambda}\ln\sigma\right] = 0\ , \qquad (3.4.9)$$

$$\left(\cos\theta + \frac{1}{\cos\theta}\right)\frac{A'}{A} = -\frac{\bar{\gamma}^2\bar{\mu}_c}{\bar{c}\lambda^2}Y_c(\Delta\phi) + \frac{\bar{\gamma}^2}{\bar{c}\lambda Y_c\sqrt{2\bar{c}\bar{R}\bar{\gamma}}} \qquad (3.4.10)$$

and

$$\frac{A_0'}{A_0} = -\frac{\bar{\alpha}^2\bar{\mu}_c}{2\bar{c}_0\lambda^2}Y_c(\Delta\phi_0) + \frac{\bar{\alpha}^2}{2\bar{c}_0Y_c\lambda\sqrt{2\bar{c}_0\bar{R}\bar{\alpha}}} + i\,\mathcal{I}m\left(\frac{A_0'}{A_0}\right)_{initial}\ . \qquad (3.4.11)$$

Equations (3.4.8) and (3.4.9) are dispersion relations which determine $\bar{\alpha}$ and $\bar{\gamma}$ in terms of $\bar{c}$ (or in terms of the scaled Strouhal number $\bar{\alpha}\bar{c}$). Since their coefficients are all real, they are consistent with our original

assertion that $\bar{\alpha}$ and $\bar{c}$ are real quantities. In fact, it follows from equations (3.7) and (3.4.8) that

$$\bar{\beta} = \frac{\sqrt{3}}{2}\bar{\alpha} + \frac{4}{\sqrt{3}}\sigma^3 \mathcal{I}m\frac{A_0'}{A_0} + O(\sigma^4) \ . \tag{3.4.12}$$

This shows that $\bar{\beta}$ and $\bar{\alpha}$ satisfy the usual long-wavelength, small-growth-rate resonance condition to within the order of the detuning. To a first approximation, equation (3.4.9) shows that $\bar{c}_0$ and $\bar{\alpha}$ satisfy the usual long-wavelength, small-growth-rate dispersion relation

$$\bar{c}_0 = \frac{\bar{\alpha}}{\bar{\lambda}} \ . \tag{3.4.13}$$

The imaginary part of the dispersion relations (i.e., the matching between zones II and III) produces the real parts of equations (3.4.10) and (3.4.11). For the initial linear growth, $\Delta\hat{\phi}$ is real. The amplitude A is real, and A_0 is initially complex, but its imaginary part remains equal to its initial value. Nonlinearity causes both amplitudes to become complex. Since the amplitudes appear as order σ^3 in the dispersion relations, the imaginary parts of A'/A or A_0'/A_0 are balanced by the imaginary part of the corresponding $\Delta\phi$. Therefore, equations (3.4.10) and (3.4.11) in their complex form are valid for both the linear and nonlinear growth regimes; they relate the (slow) growth rates of the instability waves A'/A and A_0'/A_0 to the phase jumps $\Delta\phi$ and $\Delta\phi_0$ across the critical layer. To determine these latter quantities, we must consider the flow in the critical layer.

Equations (3.2.3), (3.2.6) to (3.2.9), (3.4.5), and (3.4.6) show that the flow field in zone II can be written as

$$u = \sigma\lambda Y - \sigma^4 \frac{Y^2}{2}\left(\frac{\lambda^2}{4!} Y^2\right) + Re\left\{\left[\lambda + \sigma a_o + \sigma^3\left(f' + i\mu_c Y_c \phi_o^{\pm}\right)\right]\varepsilon A_o e^{iX} + 2\left(\frac{\lambda + \sigma a}{\cos\theta}\right.\right.$$

$$+ \frac{\bar{c}(\lambda + \sigma a)}{\lambda Y - \bar{c}} \tan\theta \sin\theta + \sigma^3\left\{f' \cos\theta + \frac{\tan\theta \sin\theta}{\lambda Y - \bar{c}}\left\{\lambda F(o) + \bar{\mu}_c \bar{c}\right.\right.$$

$$\times \left[(Y - Y_c)\ln|Y - Y_c| + Y_c \ln Y_c\right] + \lambda Y^2\left[\frac{1}{2}\mu_c - \frac{\lambda^2 Y}{4!}\left(Y_c + \frac{5}{2} Y\right.\right.$$

$$\left.\left.\left.\left.\left. - \frac{\lambda}{\lambda Y - \bar{c}} \frac{Y^2}{2}\right)\right]\right\} + \frac{\lambda A'}{\bar{\gamma} i A} \sin^2\theta\left[1 - \frac{\lambda Y}{\lambda Y - \bar{c}}\left(1 + \frac{\lambda Y}{\lambda Y - \bar{c}} \frac{1}{\cos^2\theta}\right)\right]\right.\right.$$

$$\left.\left.\left. + \frac{i\bar{\mu}_c Y_c}{\cos\theta}\left(\phi^{\pm} + \frac{\bar{c}}{\lambda Y - \bar{c}} \phi^{-} \sin^2\theta\right)\right\}\right)(\cos Z)\delta A e^{iX/2}\right\} + \ldots, \qquad (3.4.14)$$

$$v = -\sigma^2 \lambda Y \, Re\left[i\bar{\alpha}\varepsilon A_o e^{iX} + 2i\bar{\gamma}(\cos Z)\delta A e^{iX/2}\right] + \ldots, \qquad (3.4.15)$$

$$w = -2\delta(\sin\theta \sin Z) \, Re \frac{\bar{c}\lambda}{\lambda Y - \bar{c}} i A e^{iX/2} + \ldots, \qquad (3.4.16)$$

and

$$p = \sigma\bar{c}\lambda \, Re\left[\varepsilon A_o e^{iX} + 2(\cos\theta \cos Z)\delta A e^{iX/2}\right] + \ldots, \qquad (3.4.17)$$

where

$$f' = \mu_c\left(Y + Y_c \ln|Y - Y_c| + Y_c\right) - \frac{\lambda^2}{2} Y^2\left(\frac{Y_c}{4} + \frac{Y}{3!}\right). \qquad (3.4.18)$$

This solution clearly becomes singular at the critical level $Y = Y_c$ and has to be rescaled in this region.

4. CRITICAL LEVEL

As indicated in the preceding section, the solution obtained for zone II (eqs. (3.4.14) to (3.4.17)) becomes singular at the critical layer. The

appropriate transverse coordinate in this region, which matches the linear growth rate, is

$$\bar{\eta} = \frac{Y - Y_c}{\sigma^2} \tag{4.1}$$

Reid (1965) predicted the critical layer thickness of the order $(\alpha R)^{-1/3}$, which is $O(\sigma^3)$, in agreement with the scaling in equation (4.1). Introducing equation (4.1) into equations (3.4.14) to (3.4.17) and expanding the result for small $\bar{\eta}$ shows that the critical-layer solution should expand as follows:

$$u - c = \sigma^3\lambda\bar{\eta} + \sigma^6\mu_c^+ Y_c\bar{\eta} + \sigma^8\mu_c\frac{1}{2}(\bar{\eta})^2 + \delta\sigma^{-2}u_{-2} + \delta\sigma^{-1}u_{-1} + \delta u_0 + \delta\sigma u_1 + \delta\sigma^2 u_2$$
$$+ \delta\sigma^3 u_3 + \varepsilon u_0^{(o)} + \varepsilon\sigma u_1^{(o)} + \varepsilon\sigma^2 u_2^{(o)} + \varepsilon\sigma^3 u_3^{(o)} + \ldots , \tag{4.2}$$

$$\bar{v} = -\varepsilon\sigma^{-2}\bar{\alpha}\lambda Y_c \, Re\, iA_0 e^{iX} - \delta\sigma^{-2}\bar{\gamma}\lambda Y_c \, 2\cos Z \, Re\, iAe^{iX/2} + \ldots , \tag{4.3}$$

$$w = \delta\sigma^{-2}w_{-2} + \delta\sigma^{-1}w_{-1} + \delta w_0 + \delta\sigma w_1 + \delta\sigma^2 w_2 + \delta\sigma^3 w_3 + \ldots , \tag{4.4}$$

and

$$p = \varepsilon\sigma\bar{c}\lambda \, Re\, A_0 e^{iX} + \delta\sigma\bar{c}\lambda\cos\theta \, 2\cos Z \, Re\, Ae^{iX/2} + \ldots , \tag{4.5}$$

where we have set

$$v = \sigma^4\bar{v} \tag{4.6}$$

and

$$\mu_c^+ = -\frac{1}{3}\left(\frac{\lambda Y_c}{2}\right)^2 . \tag{4.7}$$

The linear analysis indicates that u_0, u_1^o, and u_0^o are independent of $\bar{\eta}$ and that

$$u_2^o = u_2 = w_0 = w_2 = 0 . \tag{4.8}$$

The linear solution ((3.4.14) to (3.4.18)) shows that the functions u_3^o and u_3 are discontinuous and singular across the critical layer. The other functions u_{-2}, u_{-1}, u_1, w_{-2}, w_{-1}, and w_1 are singular at $\bar{\eta} = 0$, and therefore, the linear solution is invalid. The full nonlinear momentum equations are thus needed to obtain a valid solution at the critical level.

The nonlinear terms in the critical-layer solution will balance the velocity jump at the same order as in the linear solution when

$$\varepsilon = \sigma^{10} \quad . \tag{4.9}$$

By substituting the expansions (4.2) to (4.5) into the full momentum equations, the latter can be expressed in terms of the scaled variables x_1, X, Z, and $\bar{\eta}$ as

$$\bar{D}\underset{\sim}{u} = -\left(\bar{\alpha}P_X + \sigma^3 P_{x_1},\ \sigma^{-8}P_{\bar{\eta}},\ \bar{\beta}P_Z\right) \tag{4.10}$$

and the continuity equation can be written as

$$\bar{\alpha}u_X + \bar{v}_{\bar{\eta}} + w_Z + \sigma^3 u_{x_1} = 0 \ , \tag{4.11}$$

where we have set

$$\bar{D} \equiv \bar{\alpha}(U - c)\frac{\partial}{\partial X} + \bar{v}\frac{\partial}{\partial \bar{\eta}} + \sigma^3 u\frac{\partial}{\partial x_1} + \bar{\beta}w\frac{\partial}{\partial Z} - \sigma^3 H\frac{\partial^2}{\partial \bar{\eta}^2} \tag{4.12}$$

and

$$\underset{\sim}{u} \equiv (u,\bar{v},w) \ . \tag{4.13}$$

The Haberman parameter

$$H = \frac{1}{R\sigma^{10}} = \frac{1}{\bar{R}} \tag{4.14}$$

is order one.

It is also convenient to work with the equation for Z-component vorticity ω, which can be written as

$$\sigma\bar{D}\omega = \bar{\beta}\left(\sigma^{-2}u_Z w_{\bar{\eta}} + \sigma\omega w_Z - \sigma^{6}\bar{\alpha}\bar{v}_Z w_X - \sigma^{9}\bar{v}_Z w_{x_1}\right) . \tag{4.15}$$

The first stage of the development of the waves, which occurs when the amplitude of the oblique waves does not exceed the order of that of the two-dimensional wave, is considered here. In this case all modal amplitudes are of the same order so that

$$\delta = \varepsilon \tag{4.16}$$

Substituting (4.16) into (4.2) to (4.5), combining terms of equal power, and substituting the resulting expansion into (4.10) and (4.13), gives

$$\mathscr{L}_o\, u_{-2} = \left(\frac{\lambda\bar{c}}{\bar{\gamma}}\right)\bar{\beta}^2\, 2\cos Z\, \mathcal{R}e\, iAe^{iX/2} , \tag{4.17}$$

$$\mathscr{L}_o\, u_1 = -\bar{c}u_{0x_1} - v_1\lambda - \left(\bar{\alpha}P_{3X} + P_{0x_1}\right) - \left(\bar{\alpha}\mu_c^{+}Y_c\bar{\eta}u_{-2X} + \lambda\bar{\eta}u_{-2x_1}\right) - \lambda Y_c^2\mu_c^{+}\, \mathcal{R}e\, E , \tag{4.18}$$

$$\mathscr{L}_o\, u_3 = -\bar{c}u_{2X_1} - v_3\lambda - \left(\bar{\alpha}P_{5X} + P_{2x_1}\right) - \left(\bar{\alpha}\mu_c^{+}Y_c\bar{\eta}\,\frac{\partial}{\partial X} + \lambda\bar{\eta}\,\frac{\partial}{\partial_{x_1}}\right)u_o$$

$$- \left[\bar{\alpha}\left(\frac{\mu_c\bar{\eta}^2}{2} + u_{-2}\right)\frac{\partial}{\partial X} - \lambda Y_c\, \mathcal{R}e\, E\,\frac{\partial}{\partial\bar{\eta}} + w_{-2}\bar{\beta}\,\frac{\partial}{\partial Z}\right]\left(\frac{\mu_c\bar{\eta}^2}{2} + u_{-2}\right) , \tag{4.19}$$

$$\mathscr{L}_o\, w_{-2} = \frac{\lambda\bar{c}}{\bar{\gamma}}\frac{\bar{\alpha}}{2}\bar{\beta}\, 2\sin Z\, \mathcal{R}e\, Ae^{iX/2} , \tag{4.20}$$

$$\mathscr{L}_o\, w_1 = -\bar{\alpha}Y_c\mu_c^{+}\bar{\eta}w_{-2X} - \lambda\bar{\eta}w_{-2x_1} - \bar{\beta}P_{3Z} - \bar{c}w_{0x_1} , \tag{4.21}$$

$$\mathscr{L}_o\, w_3 = -\bar{c}w_{2x_1} - \mu_c^+ Y_c \bar{\eta}\bar{\alpha}w_{0X} - \lambda\bar{\eta}w_{0x_1} - \bar{\beta}P_{5Z} + \lambda Y_c w_{-2\bar{\eta}}\, Re\, E$$

$$- \alpha\left(u_{-2}w_{-2X} - w_{-2}u_{-2X}\right) - \bar{\alpha}\mu_c \frac{1}{2}\bar{\eta}^2 w_{-2X} , \qquad (4.22)$$

$$\mathscr{L}_o\, u_{-2\bar{\eta}} = \beta\lambda w_{-2Z} , \qquad (4.23)$$

$$\mathscr{L}_o\, u_{1\bar{\eta}} = -\bar{c}u_{0\bar{\eta}x_1} + \lambda\left(\bar{\beta}w_{1Z} - \bar{\eta}u_{-2x_1\bar{\eta}}\right) - Y_c\mu_c^+\bar{\alpha}\left(u_{-2X} + \bar{\eta}u_{-2X\bar{\eta}}\right) , \qquad (4.24)$$

$$\mathscr{L}_o\, u_{3\bar{\eta}} = -\mu_c^+ Y_c\left(\bar{\eta}\bar{\alpha}u_{0\bar{\eta}X} - \bar{\beta}w_{0Z}\right) - \lambda\left[\bar{\eta}u_{0\bar{\eta}x_1} - \bar{\beta}w_{3Z} - Y_c\left(u_{-2\bar{\eta}\bar{\eta}} + \mu_c\right) Re\, E\right]$$

$$- \bar{\beta}\left(w_{-2}u_{-2Z} - u_{-2}w_{-2Z}\right)_{\bar{\eta}} - \bar{c}u_{2\bar{\eta}x_1} + \mu_c\bar{\beta}\left(\frac{\bar{\eta}^2}{2}\, w_{-2Z}\right)_{\bar{\eta}} , \qquad (4.25)$$

$$\bar{\alpha}u_{-2X} + \bar{\beta}w_{-2Z} = 0 , \qquad (4.26)$$

$$\bar{\alpha}u_{1X} + \bar{v}_{1\bar{\eta}} + \bar{\beta}w_{1Z} + u_{-2x_1} = 0 , \qquad (4.27)$$

and

$$\bar{\alpha}u_{3X} + \bar{v}_{3\eta} + \bar{\beta}w_{3Z} + u_{0x_1} = 0 , \qquad (4.28)$$

where

$$\mathscr{L}_o \equiv \bar{\alpha}\lambda\bar{\eta}\frac{\partial}{\partial\bar{X}} - H\frac{\partial^2}{\partial\bar{\eta}^2} \qquad (4.29)$$

and

$$E = i\left(A_0\bar{\alpha}e^{iX} + 2A\bar{\gamma}\cos Z\, e^{iX/2}\right) . \qquad (4.30)$$

These equations ultimately determine the amplitude equations. Equations for velocity components at other σ orders are not displayed here, since they do not influence the amplitude equations. The y-momentum equations indicate

that the pressure derivatives with respect to $\bar{\eta}$ are zero up to the σ^{18} order.

5. AMPLITUDE EQUATIONS

The set of equations (4.17) to (4.28) must be solved subject to the transverse boundary conditions so that they match the outer solution, equations (4.2) to (4.5). Equations (4.17) and (4.20) indicate that the lowest order solutions are given by

$$u_{-2} = 2 \tan\Theta \cos Z \, Re\left[iQ(\bar{\eta},x_1)e^{iX/2}\right] \tag{5.1}$$

and

$$w_{-2} = 2 \sin Z \, Re\, Q(\bar{\eta},x_1)e^{iX/2} , \tag{5.2}$$

where Q satisfies

$$\bar{L}_1 Q = \bar{\gamma}\lambda\bar{c}(\sin\Theta \cos\Theta)A , \tag{5.3}$$

subject to the transfer boundary condition

$$Q \to 0 \quad \text{as} \quad \bar{\eta} \to \pm\infty . \tag{5.4}$$

We have set

$$\bar{L}_n \equiv \frac{i\bar{\alpha}n}{2}\lambda\bar{\eta} - H\frac{\partial^2}{\partial\bar{\eta}^2} \quad \text{for} \quad n = 1,2 . \tag{5.5}$$

Equations (4.22), (4.23), (4.25), and (4.26) are manipulated to obtain

$$\mathcal{L}_o\, u^+_{1\bar{\eta}} = -\bar{c}u^+_{0\bar{\eta}x_1} - \alpha\mu_c^+Y_c\left(\bar{\eta}u^+_{-2}\right)_{\eta X} + \lambda D^+w_1 - \lambda\bar{\eta}u^+_{-2x_1\eta} - \lambda w_{-2x_1}\sin\Theta \tag{5.6}$$

and

$$\begin{aligned}\mathcal{L}_o\, u^+_{3\bar{\eta}} = {} & -\mu_c\bar{\eta}\left(\frac{\alpha}{2}\bar{\eta}u^+_{1\bar{\eta}X} - D^+w_1\right) + \lambda Y_c\mu_c\cos\Theta\, Re\, E - \mu_c^+Y_c\bar{\eta}\left(\alpha u^+_{0\bar{\eta}X} - D^+w_0\right) \\ & - \lambda\left(\bar{\eta}u^+_{0\eta X_1} - D^+w_3 - Y_c\, Re\, Eu^+_{-2\bar{\eta}\bar{\eta}}\right) \\ & - \left(w_{-2}D^+u_{-2} - u_{-2}D^+w_{-1}\right)_{\bar{\eta}} - \bar{c}u^+_{2\bar{\eta}x_1} ,\end{aligned} \tag{5.7}$$

where

$$u_n^+ = u_n \cos\theta + w_n \sin\theta \quad \text{for} \quad n = 1,2,3, \ldots , \tag{5.8}$$

and

$$D^+ = (\cos\theta)\bar{\beta}\frac{\partial}{\partial Z} - (\sin\theta)\bar{\alpha}\frac{\partial}{\partial X} . \tag{5.9}$$

The functions $u^+_{1\bar{\eta}}$ and $u^+_{3\bar{\eta}}$ must be expressible in the form

$$u^+_{1\bar{\eta}} = Re \sum_{m,n=0}^{3} Q^{(1)}_{n,m-1}(\bar{\eta},x_1)e^{i[(n/2)X+(m-1)Z]} \tag{5.10}$$

and

$$u^+_{3\bar{\eta}} = Re \sum_{m,n=0}^{3} Q^{(3)}_{n,m-1}(\bar{\eta},x_1)e^{i[(n/2)X+(m-1)Z]} , \tag{5.11}$$

where $Q^{(1)}_{1,1}$ satisfies the relation

$$\bar{L}_1 Q^{(1)}_{1,1} = -\lambda w_{-2x_1}\sin\theta , \tag{5.12}$$

$Q^{(3)}_{1,1}$ satisfies the relation

$$\bar{L}_1 Q^{(3)}_{1,1} = \alpha\frac{\mu_c}{2}\bar{\eta}^{-2}\frac{i}{2}Q^{(1)}_{1,1} + \lambda Y_c\left[\bar{\alpha}\sin\theta\, A_o\, Q^{*}_{\bar{\eta}\bar{\eta}} + i\mu_c\bar{\gamma}A\cos\theta\right] , \tag{5.13}$$

and $Q^{(3)}_{2,0}$ satisfies the relation

$$\bar{L}_2 Q^{(3)}_{2,0} = \cos\theta\left[i\bar{\alpha}\tan^2\theta\, Q^{2}_{\bar{\eta}} - \lambda Y_c\bar{\gamma}\left(A\tan\theta\, Q^{*}_{\bar{\eta}\bar{\eta}} - 2i\mu_c A_o\cos\theta\right)\right] . \tag{5.14}$$

Here, the asterisks denote the complex conjugate.

Examination of equations (3.4.14), (3.4.17), and (4.2) to (4.5) indicates that only $u^+_{3\bar{\eta}}$ is discontinuous across the critical layer. Therefore, it follows from equations (3.4.10), (3.4.11), and (5.11) that these solutions must satisfy

$$\int_{-\infty}^{\infty} Q_{1,1}^{(3)} d\bar{\eta} = \frac{\bar{c}\lambda^2 i}{\bar{\gamma}^2} \left[\left(\cos\theta + \frac{1}{\cos\theta} \right) A' - \frac{\lambda^2 A}{\sqrt{2}\,\bar{R}} \right] \tag{5.15}$$

and

$$\int_{-\infty}^{\infty} Q_{2,0}^{(3)} d\bar{\eta} = \frac{2\bar{c}\lambda^2 i}{\bar{\alpha}^2} \left[A_o' - \frac{\lambda^2 A_o}{2\sqrt{2}\,\bar{R}} - iA_o \mathcal{I}m\left(\frac{A_o'}{A_o} \right)_i \right] \cos\theta \tag{5.16}$$

in order to match the discontinuous $O(\sigma^{13})$ terms in equation (3.4.14). Equations (5.15) and (5.16) arise from the requirement that the changes in the fundamental and subharmonic components of the velocity across the critical layer as calculated from the external solution be the same as when they are calculated from the internal solution. This latter solution is obtained by solving equations (5.3) and (5.12) to (5.14) and by substituting the result in equations (5.15) and (5.16).

To obtain the inner solution, we introduce the following normalized variables:

$$\bar{x} = x_1 - x_o \,, \tag{5.17}$$

$$\eta = \frac{\bar{\eta}}{\bar{c}} \,, \tag{5.18}$$

$$h = \frac{2H}{\bar{\alpha}\lambda\bar{c}^3} \,, \tag{5.19}$$

where x_o is the origin of the nonlinear region. Introducing these into equations (5.3) and (5.12) to (5.14) and taking the Fourier transforms with respect to η gives

$$\hat{Q} = 2\pi(\sin\theta)A(\bar{x})H(-k)e^{hk^3/3} \,, \tag{5.20}$$

$$\frac{\partial \hat{Q}_{1,1}^{(1)}}{\partial x} = \frac{\pi}{\bar{\alpha}\bar{c}} \sin^2\theta \frac{dA}{dx_1} e^{hk^3/3} \int_{-k}^{-\infty} H(k)dk \,, \tag{5.21}$$

$$\hat{Q}^{(3)}_{1,1} = \frac{4\pi Y_c}{\bar{c}}\, e^{hk^3/3}\left[\left(\frac{\sin\theta}{\bar{c}}\right)^2 A_o(\bar{x})A^*(\bar{x}) \int_{\infty}^{k} e^{-2hk_1^3/3}\, k_1^2 H(k_1)dk_1 + i\,\frac{\mu_c}{2}\, A(\bar{x})H(-k)\right], \tag{5.22}$$

$$\hat{Q}^{(3)}_{2,0} = e^{hk^3/6}\left[\frac{4\pi\beta}{\lambda\bar{\alpha}\bar{c}^2}\left(\frac{\bar{\beta}}{\bar{\gamma}}\right)^3 A^2 \int_{\infty}^{k}\int_{-\infty}^{\infty}\int_{-\infty}^{\infty} e^{(h/3)\left(k_1^2+k_2^2\right)-\left[\left(hk_3^2\right)/6\right]}\right.$$

$$\times\, \delta(k_1 + k_2 - k_3)dk_1\, dk_2\, dk_3 - \frac{2\pi\bar{\beta}^2 Y_c}{\alpha\bar{c}^3\gamma}\, A^2 \int_0^k k_1^2 H(-k_1) e^{\left(hk_1^3\right)/6}\, dk_1$$

$$\left. + \frac{Y_c\bar{\alpha}}{\bar{\gamma}\bar{c}}\, i\pi\mu_c H(-k)\right], \tag{5.23}$$

where the notation

$$\hat{F}(k) = \int_{-\infty}^{\infty} e^{-ik\eta}\, F(\eta)d\eta \tag{5.24}$$

is used to denote the Fourier transform of any function $F(\eta)$ so that its inverse is given by

$$F(\eta) = \frac{1}{2\pi}\int_{-\infty}^{\infty} e^{ik\eta}\, \hat{F}(k)dk\ . \tag{5.25}$$

Since the integral over η is just the zero wave number component of the Fourier transform, then equation (5.15) gives

$$\left(\cos\theta + \frac{1}{\cos\theta}\right)\frac{dA}{d\bar{x}} = \frac{\lambda^2}{\sqrt{2}\,\bar{R}}\, A + 2\left(\frac{\bar{\gamma}}{\bar{\alpha}}\right)^2 N_o A + i\Gamma A^* A_o\ , \tag{5.26}$$

where

$$N_o = \frac{\pi Y_c}{2\bar{c}}\left(\frac{\bar{\alpha}}{\lambda}\right)^2 \mu_c \tag{5.27}$$

and

$$\Gamma = \pi \frac{\bar{\gamma}^2}{\bar{\alpha}^2} \frac{\bar{\alpha}^3 \bar{c}}{\lambda^2} \bar{R} \sin^2\theta \ . \tag{5.28}$$

Solving for $\hat{Q}_{2,0}$ shows that the nonlinear interaction term makes no contribution to the velocity jump integral of equation (5.16), so it follows that the fundamental amplitude A_o is still determined by the linear growth relation

$$Re \frac{A_o'}{A_o} = - \frac{\pi}{8} \frac{\bar{R}^2}{\lambda^3} + \frac{\lambda^2}{2\sqrt{2}\ \bar{R}} \ , \tag{5.29}$$

which can be integrated to give

$$\left| \frac{A_o}{a_o^o} \right| = e^{k_o \bar{x}} \tag{5.30}$$

where

$$k_o = - \frac{\pi}{8} \frac{\bar{R}^2}{\lambda^3} + \frac{\lambda^2}{2\sqrt{2}\ \bar{R}} \ . \tag{5.31}$$

This shows that the fundamental is determined by the linear growth relation

$$A_o = a_o^o e^{(k_o + i k_i)\bar{x}} \tag{5.32}$$

where a_o^o is the complex amplitude of the fundamental instability wave at $\bar{x} = 0$, and k_i is the initial wave number detuning factor, which can be chosen as an initial condition. This shows that there is no back-reaction of the oblique mode on the two-dimensional mode, and that, consequently, the two-dimensional wave follows the linear theory.

With the fundamental wave given by equation (5.32), the oblique waves' amplitude equation (5.26) is written as

$$\frac{dA}{d\bar{x}} = \frac{4}{5} k_o A + D i A_o A^* \ , \tag{5.33}$$

where

$$D = \frac{3}{10}\,\pi\,\frac{\bar{R}^3}{\lambda} \tag{5.34}$$

and the following relations are used to the order of approximation of the analysis:

$$\bar{\alpha} = \bar{\gamma}, \qquad \cos\Theta = \frac{1}{2}, \qquad \bar{c} = \frac{\bar{\alpha}}{\lambda} = \lambda Y_c = \frac{\bar{R}}{\bar{\alpha}}\ . \tag{5.35}$$

Equation (5.33) can be split into magnitude and phase equations, respectively:

$$\frac{d|A|}{d\bar{x}} = \frac{4}{5}\,k_o|A| - D\left|a_o^o\right| e^{k_o\bar{x}}\,\sin(\psi_{oi} + k_i\bar{x} - 2\tilde{\psi})|A| \tag{5.36}$$

$$\frac{d\tilde{\psi}}{d\bar{x}} = D\left|a_o^o\right| e^{k_o\bar{x}}\,\cos(\psi_o + k_i\bar{x} - 2\tilde{\psi})\ , \tag{5.37}$$

where $\tilde{\psi}$ is the phase angle of A and ψ_o is the phase angle of a_o^o. The solution of equations (5.36) and (5.37) is subject to the condition that it match with the upstream linear solution.

6. DEVELOPMENT OF AMPLITUDES WITHIN THE NONLINEAR REGION

In the nonlinear region, k_o, k_i, and $\bar{R}$ can be taken as constants. The amplitude of the two-dimensional wave follows the simple linear growth relation of equation (5.32). The solution for the oblique waves' amplitude equations (5.36) and (5.37) depends on the initial detuning factor. In section (6.1), we present an analytical solution for the case of perfect tuning, that is, $k_i = 0$. The effect of the detuning factor will be discussed in section (6.2.)

6.1. Perfect Tuning

For $k_i = 0$, the system of equations (5.36) and (5.37) can be solved analytically to obtain

$$|A| = a^{o}\exp\left(\frac{4}{5}\, k_o \bar{x}\right)\exp\left\{\frac{D}{k_o}\left|a_o^o\right| P + \frac{1}{2}\ln\left[\frac{1 + c_4\, e^{-4(D/k_o)\left|a_o^o\right| P}}{1 + c_4}\right]\right\} \tag{6.1}$$

where

$$P = e^{k_o \bar{x}}, \tag{6.2}$$

and the effective phase angle ψ_e defined as

$$\psi_e = \psi_o - 2\tilde{\psi} \tag{6.3}$$

is given by

$$\sin(\psi_e) = \frac{r - 1}{r + 1} \tag{6.4}$$

where

$$r = c_4\, e^{-4(D/k_o)\left|a_o^o\right| P}. \tag{6.5}$$

The constants a^o and c_4 are to be determined from matching with the outer linear solution $\bar{x} \to -\infty$, and c_4 can be related to the phase angle ψ_{eo} at $\bar{x} = 0$ by

$$c_4 = \frac{1 + \sin \psi_{eo}}{1 - \sin \psi_{eo}}, \tag{6.6}$$

The first exponential factor in equation (6.1) is the linear growth rate. The next exponential factor represents augmentation or suppression of the growth above the linear growth, depending on the initial phase angle ψ_{eo} (which determines c_4). Note that c_4 ranges from 0 to ∞. Two values of ψ_{eo} are of particular interest. If $\psi_{eo} = \pi/2$, $c_4 = \infty$ and equation (6.1) reduces to

$$|A| = a \exp\left(\frac{4}{5} k_o \bar{x}\right) \exp\left(\frac{-D}{k_o} \left|a_o^o\right| e^{k_o \bar{x}}\right) . \tag{6.7}$$

If $\psi_{eo} = 3\pi/2$, $c_4 = 0$ and equation (6.1) reduces to

$$|A| = a \exp\left(\frac{4}{5} k_o \bar{x}\right) \exp\left(\frac{D}{k_o} \left|a_o^o\right| e^{k_o \bar{x}}\right) . \tag{6.8}$$

For $\psi_{eo} = 3\pi/2$, the second exponential factor in equation (6.8) represents an explosive, exponential-of-an-exponential growth. Thus the resonant-triad interaction is a very powerful mechanism for augmenting the growth rate of the oblique instability waves that propagate at an angle of 60° to the downstream direction.

The amplitude of the oblique waves in the nonlinear region (eqs. (6.1) and (6.4)) at various initial phase angles ψ_{eo} is shown in figure 4 for $\left|a_o^o\right| = 1$ and $\bar{R} = 0.8\, \bar{R}_{up}$, where $\bar{R}_{up}$ is the upper-branch scaled Reynolds number. Figure 4(a) shows that the amplitude grows explosively for $\psi_{eo} = 3\pi/2$, as given by equation (6.8). The trend is reversed when $\psi_{eo} = \pi/2$ (eq. (6.7)). The phase of the amplitude is shown in figure 4(b). If $\psi_{eo} = \pi/2$ or $3\pi/2$, the effective phase angle ψ_e remains at its initial value. If $\psi_{eo} = 0$ or π, the effective phase angle develops rapidly to an asymptotic value of $\psi_e = 3\pi/2$.

6.2. Effect of Detuning Factor

Since perfect tuning may not always be achieved, we discuss here the effect of the initial detuning factor k_i. The magnitude of the plane wave's amplitude, equation (5.32), is independent of the detuning factor. The detuning factor causes the phase angle of the plane wave to vary linearly in $\bar{x}$. The effect of the detuning factor on the oblique waves is obtained by solving equations (5.36) and (5.37) numerically for several values of k_i; the results are shown in figure 5. Only large values of k_i, compared to k_o, can

influence the solution. Figure 5(a) shows that detuning only moves the location of the resonant amplification downstream; however, detuning causes the effective phase angle to vary in the upstream linear region, as figure 5(b) indicates. But the effective phase angle reaches its optimum value of $\sin \psi_e = -1$ some distance downstream, which allows for the explosive growth to occur. This can be understood by noting that the solution of equation (5.37) is independent of that of equation (5.36), and that the former can be written as

$$\frac{dx_i}{dx} = k_i - 2D\left|a_o^o\right| e^{k_o \bar{x}} \cos x_i \tag{6.9}$$

where

$$x_i = \psi_o + k_i \bar{x} - 2\tilde{\psi} \ . \tag{6.10}$$

For large $\bar{x}$ values, equation (6.9) reduces to that of perfect tuning. Thus, for $\psi_{eo} = 270°$, if $k_i = 0$, $\sin \psi_e = -1$ is achieved immediately at $\bar{x} = 0$. As k_i increases, the optimum angle is achieved farther downstream. The nonlinear contribution to equation (5.36) is dependent on k_i in $\sin(x_i)$. Since $\sin(x_i)$ reaches the optimum value at some downstream location that increases with k_i, the only effect of k_i on the amplitude is to move down the location of resonance amplification. Since for reasonable values of k_i the effect of detuning is thus negligible, the solution at $k_i = 0$ can be considered a good approximation. Therefore, in the following sections, where the composite solution and the results are presented, we assume $k_i = 0$ and use the analytical solution (eqs. (6.1) to (6.5)).

7. COMPOSITE SOLUTION

The overall instability-wave growth is strongly dependent on both the nonlinear effects discussed here and the weakly nonparallel effects. In order to incorporate both effects into a single formula, we use the composite

expansion as suggested by Van Dyke (1975). The composite expansion is formed from the present inner solution A_{in} and the slowly varying outer solution A_{out}. Here the composite solution for the case of perfect tuning, that is, $k_i = 0$, is presented. In section 7.1 the composite expansion in the unscaled coordinate x, which is the dimensional streamwise coordinate normalized by the local boundary-layer thickness, is obtained. In section 7.2 the integrals that depend on the boundary-layer variations are evaluated and the solution is presented in terms of the unscaled boundary-layer coordinates.

7.1. Composite Expansion of the Two-Dimensional Wave and Oblique Waves

Consider first the plane wave. The outer linear solution can be written as

$$A_{o,out} = A_o^o(x_2) e^{\sigma^4 \int_0^x k_o(x_2)dx} \tag{7.1}$$

where x_2 is the slowly varying boundary-layer variable. The origin of the disturbances is at $x = 0$ (see fig. 2). As $x_2 \to x_o$, this outer solution can be approximated by

$$A_{o,out} \to a_o^o e^{k_o \bar{x}} = A_{o,i/o} \tag{7.2}$$

where

$$a_o^o = A_o^o(o) e^{\sigma^4 \int_0^{x_o} k_o d_x} . \tag{7.3}$$

Consider the inner solution of the plane wave (eq. (5.32)) as $\bar{x} \to -\infty$; the solution can be written as

$$A_{in} \to a_o^o e^{k_o \bar{x}} = A_{o,in/out} . \tag{7.4}$$

The composite solution is given according to van Dyke (1975) as

$$A_c = \frac{A_{o,in} A_{o,out}}{A_{o,in/out}} \quad . \tag{7.5}$$

Thus, for the plane wave, the composite solution is given by

$$A_{o,c} = A_o^o(o) e^{\sigma^4 \int_0^x k_o(x_2)dx} \tag{7.6}$$

and we have approximated $A_o^o(x_2)$ by

$$A_o^o(x_2) = A_o^o(x = 0) \tag{7.7}$$

The composite solution for the plane wave (eq. (7.6)) is thus the same as its outer solution. This is an expected result since the two-dimensional wave in the nonlinear region is still given by its linear solution.

With respect to the oblique waves, the outer solution is given by

$$A_{out} = A^o(x_2) e^{(4/5)\sigma^4 \int_0^x k_o dx} \quad . \tag{7.8}$$

As $x_2 \to x_o$, this outer solution can be written as

$$A_{out} \to a\, e^{(4/5)k_o \bar{x}} = A_{in/out} \tag{7.9}$$

where

$$a = A^o(o) e^{(4/5)\sigma^4 \int_0^{x_o} k_o dx} \quad . \tag{7.10}$$

The inner solution for the oblique waves, equations (6.1) to (6.4), can be written as

$$A_{in} = a\, e^{(4/5)k_o \bar{x}} g(\bar{x}) \tag{7.11}$$

where

$$g(\bar{x}) = \exp\left[T + \frac{1}{2}\ln\left(\frac{1 + c_4 e^{-4T}}{1 + c_4}\right)\right] e^{i\tilde{\psi}} , \tag{7.12}$$

$$T = \frac{D}{k_o}\left|a_o^o\right| e^{k_o \bar{x}} , \tag{7.13}$$

$$\sin(\psi_o - 2\tilde{\psi}) = \frac{r - 1}{r + 1} , \tag{7.14}$$

and

$$r = c_4 e^{-4T} . \tag{7.15}$$

As $\bar{x} \to -\infty$,

$$A_{in} \to a\, e^{(4/5)k_o \bar{x}} = A_{in/out} . \tag{7.16}$$

The composite solution

$$A_c = \frac{A_{in} A_{out}}{A_{in/out}} \tag{7.17}$$

is then given by

$$A_c = A^o(o) e^{(4/5)\sigma^4 \int_0^x k_o dx}\, g(\bar{x}) e^{i\tilde{\psi}} , \tag{7.18}$$

where $A^o(x_2)$ has been approximated by

$$A^o(x_2) = A^o(x = 0) . \tag{7.19}$$

We allow the coordinate system origin shift x_o to occur naturally by rewriting equation (7.13) as

$$T = \int_{-\infty}^{\bar{x}} D\left|a_o^o\right| e^{k_o \bar{x}}\, a\bar{x} . \tag{7.20}$$

Substituting for $\left|a_o^o\right|$ from equation (7.3), we obtain

$$T = \sigma^4 \left| A_o^o(x = 0) \right| \int_0^x D\, e^{\sigma^4 \int_0^x k_o dx}\, dx \ . \qquad (7.21)$$

The constant c_4, equation (7.15), is given by

$$c_4 = \frac{1 + \sin \psi_{oi}}{1 - \sin \psi_{oi}} \qquad (7.22)$$

where ψ_{oi} is the initial phase angle of the fundamental.

7.2. Composite Solution in Unscaled Boundary-Layer Coordinates

Here the solution of the amplitude functions in the unscaled boundary-layer coordinates is presented. The composite solutions (eqs. (7.16) and (7.18)) can be integrated once the boundary-layer variation with x is given. Let

$$I = \sigma^4 \int_0^x k_o(x_2) dx \qquad (7.23)$$

where $k_o(x_2)$ is given by equation (5.31) and x is normalized by the local boundary-layer thickness δ^*. If δ_o^* is the boundary thickness at $x = 0$, we can write

$$\bar{R} = \bar{R}_i \frac{\delta^*}{\delta_o^*} \qquad (7.24)$$

where $\bar{R}_i$ is the scaled Reynolds number at $x = 0$. If x_w is the distance between the leading edge of the flat plate and the origin of the disturbances $x = 0$, then according to Schlichting (1955), we can write

$$\frac{\delta^*}{\delta_o^*} = \sqrt{\frac{x_d}{x_w} + 1} \qquad (7.25)$$

where x_d is the dimensional streamwise coordinate. Equation (7.23) can be integrated to obtain

$$I = \sigma^4 R_i \left\{ -\frac{\pi}{24} \frac{\bar{R}_i}{\lambda^3} \left[\sqrt{x^\dagger + 1}\,(x^\dagger + 4) - 4 \right] + \frac{\lambda^2}{4\sqrt{2}} \frac{1}{\bar{R}_i} \left[\ln(x^\dagger + 1) + \frac{x^\dagger}{x^\dagger + 1} \right] \right\} , \tag{7.26}$$

where

$$x^\dagger = \frac{x}{x_w} \tag{7.27}$$

As in Goldstein and Durbin (1986), the scaling parameter σ can be replaced by the dimensionless frequency F^*, defined as

$$F^* = \frac{\omega \nu}{U_\infty^2} = \sigma^{12} , \tag{7.28}$$

and equation (7.26) can be written as

$$I = -\frac{\pi}{24} \frac{R_i^3 F^{*2}}{\lambda^3} \left[(x^\dagger + 4)\sqrt{x^\dagger + 1} - 4 \right] + \frac{\lambda^2}{4\sqrt{2}} \frac{1}{\sqrt{F^*}} \left[\ln(x^\dagger + 1) + \frac{x^\dagger}{x^\dagger + 1} \right] . \tag{7.29}$$

The composite solutions are now written as

$$\left| A_o \right| = \left| A_o^o \right| e^I , \tag{7.30}$$

$$|A| = A^o e^{(4/5)T} g(T) , \tag{7.31}$$

and

$$\sin \psi_e = \frac{c_4 e^{-4T} - 1}{c_4 e^{-4T} + 1} , \tag{7.32}$$

where $g(T)$ is defined in equation (7.12). From equation (7.21), T can now be written in terms of the boundary-layer coordinates as

$$T = (F^*)^{0.333}\left|A_o^o\right|R_i \int_0^{x^\dagger} \frac{1 + 0.5x^\dagger}{(1 + x^\dagger)^{3/2}} De^I dx^\dagger \ . \tag{7.33}$$

The coordinate $x^\dagger$ can be replaced by the local Reynolds number since

$$x^\dagger = \left(\frac{R}{R_i}\right)^2 - 1 \ . \tag{7.34}$$

The scaled initial amplitudes A^o and A_o^o can be related to the unscaled amplitudes A_n^o and $A_{o,n}^o$ by

$$A_n^o = F^{*10/12}A^o \tag{7.35}$$

and

$$A_{o,n}^o = F^{*10/12}A_o^o \ . \tag{7.36}$$

8. RESULTS AND DISCUSSION

Results are presented here for the development of the fundamental and the subharmonic waves as given by equations (7.30) to (7.32). The solution of these equations is dependent on the initial levels of the fundamental and subharmonics and on the initial phase-difference angle between the two-dimensional mode and the oblique modes. These factors, among others, will be discussed here.

8.1. Effect of Initial Level of the Fundamental

Figure 6 shows the amplitudes of the fundamental and the subharmonic waves normalized by the initial level of the fundamental. The normalized frequency $F^* = 10^{-5}$, and the initial phase angle ψ_{oi} is $3\pi/2$. The unscaled initial level of the subharmonic is fixed at 10^{-8}, whereas the unscaled initial level of the fundamental is varied between 10^{-5} and $10^{-2.5}$. Since the fundamental behaves linearly, as indicated herein, the figure shows that the amplification

of the fundamental is independent of its initial level. The development of the fundamental is also independent of that of the subharmonic. Kachanov and Levchenko (1984) have indicated that the development of the fundamental wave does not depend on the subharmonic development in an initial region of the amplification of small priming subharmonic fluctuations. Their results indicate no back-reaction on the fundamental up to a fundamental's initial level of 0.218×10^{-2}, which is consistent with the present results.

In this analysis, the subharmonic does not initially react back on the fundamental. This allows the fundamental to grow according to the linear theory. On the other hand, the subharmonic grows as the exponential-of-an-exponential, as figure 6 shows. This is consistent with the observations of Kachanov and Levchenko (1984), Saric, Kozlov, and Levchenko (1984), and Corke and Mangano (1989). This growth of the subharmonic is dependent on the growth of the fundamental, which acts as the catalyst for the resonant growth. The growth of the subharmonic waves increases with increasing fundamental initial amplitude, and as figure 6 indicates, the subharmonic saturates with the fundamental's decay.

8.2. Effect of Initial Level of the Subharmonic

An interesting feature of the present analysis is that the subharmonic amplitude is given by a linear function in A. The ratio A/A^{o} and the amplification rates are thus independent of the initial level of the subharmonic. The role of the initial amplitude of the subharmonic is clearly shown in the experiments of Saric et al. (1984) and Kachanov and Levchenko (1984, fig. 14(c)) in the case of simultaneous ribbon excitation at Tollmein-Schlichting frequency and its subharmonic. In the experiment, the initial level of the subharmonic was varied sinusoidally. This resulted in an amplitude A of the amplified subharmonic, which varied sinusoidally as the

initial disturbance and was proportional to the initial amplitude of the phase-locked component of the ribbon excitation. This indicates that the growth of the subharmonic is linearly dependent on the initial level of the subharmonic, which is consistent with the present analysis.

8.3. Effect of Initial Phase-Difference Angle

The magnitude of the fundamental's amplitude, which is governed by a linear process, is not dependent on the phase angle, as equation (7.6) indicates. On the other hand, the amplitude of the subharmonic, equation (7.31), is dependent on the constant c_4. This constant is determined via the initial phase angle, ψ_{oi}, by using equation (7.22). Thus, the nonlinear process is dependent on the initial phase angle ψ_{oi} between the fundamental and the subharmonic.

The effect of ψ_{oi} on the growth of the subharmonic is shown in figure 7. The effective phase angle ψ_e controls the sign of the nonlinear term in the subharmonic's amplitude equation (5.34). For $\psi_{oi} = \pi/2$ or $3\pi/2$, equation (7.31) reduces to

$$|A| = A^o \, e^{(4/5)I} \, e^{\pm T} , \qquad (8.3.1)$$

where the negative sign is for $\psi_{oi} = \pi/2$ and the positive sign is for $\psi_{oi} = 3\pi/2$. The nonlinear effects can thus amplify or reduce the growth rate, depending on the initial phase angle. The amplitude of the subharmonic at $R/R_i = \sqrt{2}$ is shown in figure 7(b) as a function of ψ_{oi}. The figure shows that, except in the vicinity of $\psi_{oi} = \pi/2$, the amplitude is close to its maximum value, which occurs at $\psi_{oi} = 3\pi/2$.

If $\psi_{oi} = 3\pi/2$, equation (7.22) shows that $c_4 = 0$ and thus equation (7.33) gives $\sin \psi_e = -1$ irrespective of x. If $\psi_{oi} = \pi/2$, c_4 is infinity and ψ_e is also a fixed value independent of x, equation (7.33) gives $\sin \psi_e = 1$. If ψ_{oi} is not close to $\pi/2$, c_4 is finite and, as x

increases, ψ_e reaches an asymptotic value $\sin \psi_e = -1$. Thus, except for $\psi_{oi} = \pi/2$, $\sin \psi_e$ tends to be -1 as x increases; these results are demonstrated in figure 8. The sign of the nonlinear term in the oblique waves' amplitude equation (5.36) is determined by $\sin \psi_{oi}$. Thus, except for $\psi_{oi} \approx \pi/2$, the amplitude of the subharmonic is close to its value of $\psi_{oi} = 3\pi/2$, as was shown in figure 7(b).

In free-shear flows, the dependence of the subharmonic amplification on the initial phase difference was observed and studied by several researchers. The analysis of Monkewitz (1988) and the numerical simulations of Patnaik, Sherman, and Corcos (1976) and Riley and Metcalfe (1980) for vortex pairing in two-dimensional mixing layers, showed that the pairing process depends on the phase difference between the fundamental and subharmonic instability waves. In the experiment of Zhang, Ho, and Monkewitz (1985) for a two-dimensional shear layer under bimodal excitation, significantly different merging patterns were observed as a result of changing the initial phase difference between the fundamental and the subharmonic. For a round jet under fundamental-subharmonic excitation, Mankbadi (1986) showed that the initial growth rate of the subharmonic is highest when the two waves are in phase. The effect of phase difference on the subharmonic's peak was found to depend on the Strouhal-number pair. For a round jet under two frequency excitations, Mankbadi, Raman, and Rice (1990) demonstrated that the interaction between the fundamental and subharmonic waves depends on an effective phase angle identical to the one defined here in equation (6.3).

For boundary layers, Klebanoff and Tidstrom (1959) showed that the disturbance grew to a large amplitude, which appears not to be qualitatively reproducible. This can be explained by the present analysis, which indicates that these high peaks may or may not occur, depending on ψ_{oi}. Since no

control was exercised over ψ_{oi} in Klebanoff and Tidstrom's (1959) experiment, it could vary at random. The analysis herein showed that if ψ_{oi} was optimum, peaks were observed, and if ψ_{oi} was close to $\pi/2$, then peaks were not observed; thus, the variation of the initial phase-difference angle can explain why the observed peaks were not reproducible.

For the case of resonant amplification of controlled subharmonic priming oscillations, Kachanov and Levchenko (1984, p. 231) observed that resonance occurs at a given phase shift ψ_r between the crests of the fundamental wave and the subharmonic. They also reported that Zelman and Maslennikova's (1982) numerical results showed the same feature. Zelman and Maslennikova (1982) calculated the growth of the waves at various initial phase shifts between the subharmonic and fundamental. The results of their calculations show that when an initial phase of the subharmonic minus the resonant phase, measured on the cycle of the subharmonic, is 90° (or 180° measured on the cycle of the fundamental), the subharmonic not only fails to grow, but it also damps with approximately the same rate as the amplification at ψ_r. Other things being equal, the damped subharmonic lags behind the subharmonic having $\psi_{oi} = \psi_r$ by an order of magnitude or more in amplitude. These numerical results are consistent with those obtained herein (fig. 7(a)) for the cases of $\psi_{oi} = \pi/2$ and $3\pi/2$, where the difference between the two values is π on the fundamental cycle or $\pi/2$ on the subharmonic cycle, as in the numerical simulations.

8.4. Nonlinear Function

The nonlinear function g in equation (7.32) is the ratio of the nonlinear amplitude to the linear amplitude. This function, defined in equation (7.12), can be written for $\psi_{oi} = 3\pi/2$ as

$$|g| = \exp\left[\frac{0.3\,\pi}{\lambda}\left|A_o^o\right|\bar{R}_{up}^{\,4}\,\frac{\ell^4}{\sqrt{F^*}}\int_0^{x^\dagger}\frac{1+0.5x^\dagger}{(1+x^\dagger)^{3/2}}\,e^I dx^\dagger\right] . \qquad (8.1)$$

Here, $\bar{R}_{up}$, which is equal to 0.1537, is the upper-branch scaled Reynolds number based on the linear theory. The location ℓ is defined by

$$\ell = \frac{\bar{R}_i}{\bar{R}_{up}} \qquad (8.2)$$

where $\bar{R}_i$ is the initial Reynolds number. Thus, $\ell < 0$ corresponds to the location of the origin of the disturbances (e.g., vibrating wire) ahead of the upper branch of the linear neutral curve, and $\ell > 1$ corresponds to a location of the origin of disturbances beyond the upper branch of the neutral curve (i.e., in the linear stable region). Other parameters being the same, equation (8.1) indicates the nonlinear interaction increases with the initial Reynolds number, R_i. Also, as shown in figure 6, the nonlinear interaction increases with $\left|A_o^o\right|$, which reaches its maximum at the upper branch. These two factors explain why the observed subharmonic resonance occurs at or beyond the upper branch.

The effect of frequency on the nonlinear function is shown in figure 9, which indicates that the nonlinear effects increase considerably with decreasing the frequency. Note that the argument of the exponent I in equation (8.1) also increases with decreasing frequency, as given by equation (7.29). Thus, the nonlinear interactions are quite sensitive to the normalized frequency F^*. Since low values of F^*, correspond to higher transitional Reynolds numbers, the present nonlinear phenomenon is particularly significant at high-Reynolds-number flows.

8.5. Nonlinear Upper Branch of Neutral Curve

Because of the nonlinear effects, the subharmonic can continue to grow beyond the upper branch of the neutral curve. The amplification factor for the oblique waves, based on the linear theory, is $0.8k_o$, whereas $0.8I$ is that which accounts for the variation of the boundary-layer thickness. However, the total amplification rate of the oblique modes is given by the sum of the linear and nonlinear amplifications. For $\psi_{oi} = 3\pi/2$, the nonlinear upper branch of the neutral curve for the oblique modes can be obtained from equation (7.31) by setting

$$0.8I + T = 0 \ , \tag{8.3}$$

which can be written as

$$0.8I + \frac{0.3\ \pi}{\lambda} \left|A_o^o\right| \bar{R}_{up}^{\ 4} \frac{\ell^4}{\sqrt{F^*}} \int_0^{x^\dagger} \frac{1 + 0.5x^\dagger}{(1 + x^\dagger)^{3/2}} e^I dx^\dagger = 0 \ . \tag{8.4}$$

The solution of this equation determines the location of the nonlinear upper branch. This equation indicates that the nonlinear neutral curve is dependent on the initial Reynolds number as well as on the initial level of the fundamental. The first term in equation (8.4) is the linear growth rate of the subharmonic, which includes the small nonparallel flow effects. The second term is the nonlinear contribution to the neutral curve. As $A_o^o \to 0$, the nonlinear contribution vanishes, and the nonlinear curve coincides with the linear one.

Since the nonlinear contribution in the upper-branch equation (8.4) is always positive for nonzero values of A_o^o, nonlinear effects extend the critical Reynolds number. Thus, depending on A_o^o and R_o, the upper branch of the neutral curve can be eliminated. Goldstein and Durbin (1986) have pointed out that nonlinear critical layers eliminate the upper branch of spatially

growing Tollmein-Schlichting waves. Figure 10 shows both the linear and the nonlinear upper branches of the neutral curves for the subharmonic. The boundary-layer growth is accounted for in both curves $\left(A^{o}_{o,n} = 0.001 \text{ and } R_i/R_{up} = 0.8\right)$. The figure shows that at high frequencies the two curves approach each other. But at low frequencies the nonlinear upper branch's Reynolds number is much larger than that of the linear one. The upper-branch Reynolds number can be increased further by increasing the initial level of the fundamental. Thus, at low frequencies, the upper branch is practically eliminated, so an initially linear stability wave can encounter nonlinear effects that cause a state of suspended, nondecaying waves, as in the fully turbulent case.

9. DETAILED COMPARISON WITH EXPERIMENTS

The results presented in section 8 are in qualitative agreement with the available data. Further detailed comparisons with the data of Kachanov and Levchenko (1984) and Corke and Mangano (1987) are presented in this section. In figures 11 to 13 the amplitudes of the two-dimensional and oblique waves are compared with the corresponding experimental data. In calculating these amplitudes, the initial amplitudes and Reynolds numbers were taken to be the same as in the experiment.

Figure 11 shows the calculated amplitudes at $F^* = 137\times10^{-6}$ compared with Kachanov and Levchenko's (1984) experimental data. The figure shows excellent agreement in the initial region. Further downstream, for $R > 600$, the measured amplitude of the oblique waves is less than the calculated one. Figures 12 and 13 show the calculated amplitudes at other frequencies and initial conditions compared with the corresponding data of Corke and Mangano (1987). These figures also show an excellent agreement for the initial development of the waves. The plane wave grows almost at its linear growth

rate. But both theory and observations show considerable growth of the oblique waves beyond that of the linear theory. At points downstream, the measured amplitude of the oblique waves is less than the predicted one. Since the amplitude of the subharmonic exceeds that of the fundamental, the disturbed flow enters a higher amplitude regime, and rescaling of the amplitudes is required. The present theory thus successfully predicts the initial resonance of the oblique waves. When the amplitude of the oblique waves exceeds that of the two-dimensional wave, a second mechanism comes into effect that reduces the growth of the oblique waves.

10. CONCLUDING REMARKS

The nonlinear interactions between a two-dimensional fundamental stability wave and a pair of oblique subharmonic waves of equal and opposite propagation angles were studied by using low-frequency scaling. Attention was focused on the initial stage of the nonlinear development of the waves. The present analysis indicated that the two-dimensional fundamental mode growth was given by the linear theory, whereas the subharmonic oblique modes grew explosively as the exponential-of-an-exponential. The fundamental acted as a catalyst for the growth of the subharmonic; therefore, the nonlinear growth of the subharmonic increased with an increase in the initial level of the fundamental.

The development of the subharmonic was found to be dependent on the initial phase-difference angle between the two-dimensional fundamental mode and the oblique subharmonic modes. For the case of perfect tuning, the optimum initial phase difference was $3\pi/2$, measured on the cycle of the fundamental. If the initial phase difference was changed π from its optimum value, the subharmonic not only failed to grow, but decayed at a rate almost equal to its amplification rate for the optimum initial phase-difference angle.

The nonlinear growth of the subharmonic increased as the nondimensional frequency F^* decreased. Thus, the present triad interactions are stronger at lower frequencies. Keeping other parameters the same, the nonlinear interaction increases with Reynold's number. Nonlinear effects tended to increase the upper-branch Reynolds number of the oblique modes. At low frequencies, the upper branch of the neutral stability curve for the oblique modes was practically eliminated.

Detailed comparisons with available data indicated that the present analysis successfully predicts the initial resonance of the oblique waves. If the subharmonic was not much larger than that of the fundamental, both theory and observations indicated that the fundamental grew according to the linear theory while the subharmonic grew at rates much higher than that predicted by the linear theory. The strong agreement between theory and experiment here has established the origin of the subharmonic resonance and of the observed three-dimensionality of the flow at boundary-layer transition.

APPENDIX

In this appendix we list the numerical coefficients that appear in (3.3.9).

$$J_1 \equiv \int_0^\infty \left[U_B^2 - \frac{1}{U_B^2} + \frac{1}{(\lambda y)^2} \right] dy \ . \tag{A-1}$$

$$J_2 \equiv -\int_0^\infty \left[\frac{1}{U_B^3} - \frac{2}{U_B^2} + U_B - \frac{1}{(\lambda y)^3} + \frac{2}{(\lambda y)^2} \right] dy \ . \tag{A-2}$$

$$J_3 \equiv \int_0^\infty \left[1 - \frac{3}{U_B^4} + \frac{8}{U_B^3} - \frac{6}{U_B^2} + \frac{3}{(\lambda y)^4} - \frac{8}{(\lambda y)^3} + \frac{6}{(\lambda y)^2} + \frac{1}{4\lambda^3 y(y+1)} \right] dy \ . \tag{A-3}$$

$$J_4 \equiv 2 \int_0^\infty U_B^2 \int_0^\infty \left(U_B^2 - \frac{1}{U_B^2} \right) dy \, dy \ . \tag{A-4}$$

$$J_5 \equiv \lim_{\substack{y \to 0 \\ \hat{c} \to 0 \\ U \to U_B}} \left(\frac{\partial \Omega_1}{\partial \hat{c}} + \lambda \Omega_2 \right) \ . \tag{A-5}$$

REFERENCES

Corke, T.C. & Mangano, R.A. 1987 Transition of a boundary layer: controlled fundamental-subharmonic interactions. In Fluid Dynamics Center Rept. No. 87-1, Illinois Institute of Technology, Chicago, Illinois.

Corke, T.C. & Mangano, R.A. 1989 Resonant growth of three-dimensional modes in transitioning Blasius boundary layers. J. Fluid Mech. 209, 93.

Cornelius, K.C. 1985 Three-dimensional wave development during boundary-layer transition. Lockheed Georgia Res. Rep. LG85RR0004, Marietta, Georgia.

Craik, A.D.D. 1971 Non-linear resonant instability in boundary layers. J. Fluid Mech. 50, 393-413.

Craik, A.D.D. 1978 Evolution in space and time of resonant wave triads. II. A class of exact solutions. Proc. R. Soc. London A 363, 257-269.

Craik, A.D.D. 1985 Resonant interactions in shear flows. In Laminar-Turbulent Transition, (ed., V.V. Kozlov), Springer, pp. 1-8.

Croswell, J.W. 1985 On the energetics of primary and secondary instabilities in plane poiseuille flow. MS Thesis, Virginia Polytechnic Institute State University, Blacksburg, VA.

DeVilliers, J.M. 1975 Asymptotic solutions of the Orr-Sommerfeld equation, Phil. Trans. Roy. Soc. of London, vol. 280, A 1295, pp. 271-316.

Drazin, P.G. & Reid, W.H. 1981 Hydrodynamic Stability. Cambridge University Press.

Eagles, P.M. 1969 Composite series in the Orr-Sommerfeld problem for symmetric channel flow, Quart. Journ. Mech. and Applied Math., vol. XXII, pt. 2, pp. 129-182.

Fraenkel, L.E. 1969 On the method of matched asymptotic expansions. Proc. Camb. Phil. Soc. 65, 209-231.

Goldstein, M.E. & Durbin, P.A. 1986 Nonlinear critical layers eliminate the upper branch of spatially growing Tollmein-Schlichting waves. Phys. Fluids 29, 2344-2345.

Goldstein, M.E., Durbin, P.A., & Leib, S.J. 1987 Roll-up of vorticity in adverse-pressure-gradient boundary layers. J. Fluid Mech. 183, 325-342.

Graebel, W.P. 1966 On determination of the characteristic equations for the stability of parallel flow, J. Fluid Mechanics, vol. 24, pt. 3, pp. 497-508.

Haberman, R. 1972, Critical Layers in Parallel Shear Flows. Stud. Appl. Math. 51, 139-161.

Herbert, Th. 1988 Secondary instability of boundary layers. In Annual Review of Fluid Mechanics, Vol. 20, (eds. J.L. Lumley, M. van Dyke, & H.L. Reed), Annual Reviews Inc., pp. 487-526.

Hultgren, L.S. 1987 Higher eigenmodes in the Blasius boundary-layer stability problem. Phys. Fluids 30, 2947-2951.

Kachanov, Yu.S., Kozlov, V.V., & Levchenko, V.Ya. 1978 Nonlinear development of a wave in a boundary layer. Fluid Dyn. 12, 383-390.

Kachanov, Yu.S. & Levchenko, V.Ya. 1984 The resonant interaction of disturbances at laminar-turbulent transition in a boundary layer. J. Fluid Mech. 138, 209-247.

Klebanoff, P.S. & Tidstrom, K.D. 1959 Evolution of amplified waves leading to transition in a boundary layer with zero pressure gradient. NASA TN D-195.

Klebanoff, P.S., Tidstrom, K.D., & Sargent, L.M. 1962 The three-dimensional nature of boundary-layer instability. J. Fluid Mech. 12, 1-34.

Landahl, M.T. 1972 Wave mechanics of breakdown. J. Fluid Mech. 56, 775-802.

Lin, C.C. 1955 The Theory of Hydrodynamic Stability. Cambridge University Press.

Mankbadi, R.R. 1986 The effect of phase-difference on the spreading rate of a jet. AIAA J. 24, 1941-1948.

Mankbadi, R.R., Raman, G. & Rice, E.J. 1990 Development of the Phase Angles of Instability Waves in Turbulent jets, AIAA paper number 90-503, Aerospace Sciences Meeting, Jan. 8-11, 1990, Reno, Nevada.

Miles, J.W. 1962 A note on the inviscid Orr-Sommerfeld equation. J. Fluid Mech. 13, 427-432.

Monkewitz, P.A. 1988 Subharmonic resonance, pairing and shredding in the mixing layer. J. Fluid Mech. 188, 223-252.

Patnaik, P.C., Sherman, F.S., & Corcos, G.M. 1976 A numerical simulation of Kelvin-Helmholtz waves of finite amplitude. J. Fluid Mech. 73, 215-240.

Reid, W.H. 1965 The stability of parallel flows. In Basic Developments in Fluid Dynamics, (ed., M. Holt), Academic Press, pp. 249-308.

Riley, J.J. & Metcalfe, R.W. 1980 Direct numerical simulation of a perturbed, turbulent mixing layer. AIAA Paper 80-0274.

Saric, W.S., Carter, J.D., & Reynolds, G.A. 1981 Computation and visualization of unstable-wave streaklines in a boundary layer. Bull. Am. Phys. Soc. 26, 1252.

Saric, W.S., Koslov, V.V., & Levchenko, V.Ya. 1984 Forced and unforced subharmonic resonance in boundary layer transition. AIAA Paper 84-0007.

Schlichting, H. 1955 Boundary Layer Theory. McGraw-Hill.

Singer, B.A., Ferziger, J.H., Spalart, P.R., & Reed, H.L. 1987 Local intermodal energy transfer of the secondary instability in a Plane Channel. AIAA Paper 87-1202.

Squire, H.B. 1933 On the stability for three-dimensional disturbances of viscous fluid flow between parallel walls. Proc. R. Soc. London A 142, 621-628.

Thomas, A.S.W. & Saric, W.S. 1981 Harmonic and subharmonic waves during boundary-layer transition. Bull. Am. Phys. Soc. 26, 1252.

Usher, J.R., Craik, A.D.D., & Hendriks, F. 1975 Nonlinear wave interactions in shear flows. Part 2. Third-order theory. J. Fluid Mech. 70, 437-461.

van Dyke, M.D. 1975 Perturbation Methods in Fluid Mechanics. Parabolic Press.

Zelman, M.B. & Maslennikova, I.I. 1982 In instability of sub- and supersonic flows (ed. V.Ya. Levchenko), pp. 5-15. ITPM SO AN SSSR, Novosibirssk (in Russian).

Zhang, Y.Q., Ho, C.M., & Monkewitz, P. 1985 The mixing layer forced by fundamental and subharmonic. In Laminar-Turbulent Transition (ed. V.V. Kozolov), Springer-Verlag, pp. 385-396.

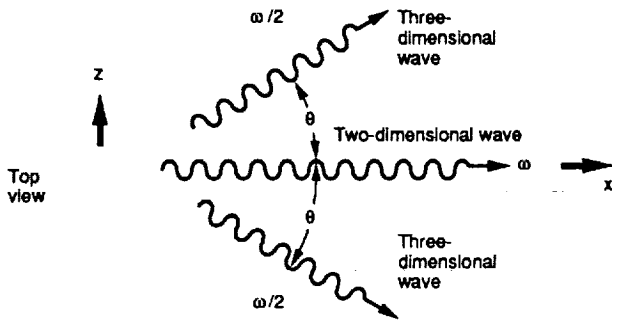

Figure 1.—Resonant triad.

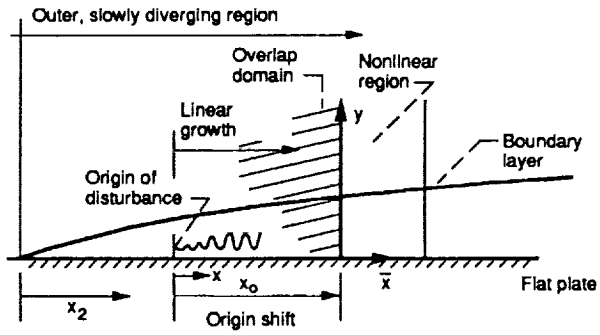

Figure 2.—Flow structure.

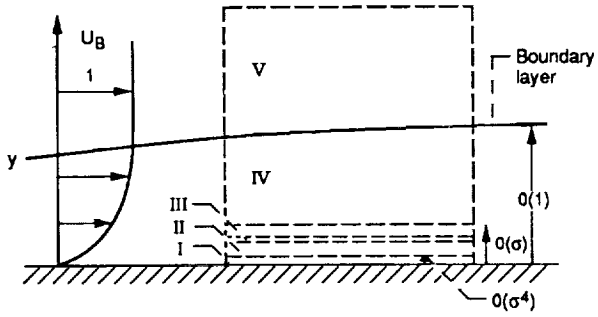

Figure 3.—Diagram for upper-branch stability structure (zones I to V) for Blasius boundary layer; U_B = Blasius velocity.

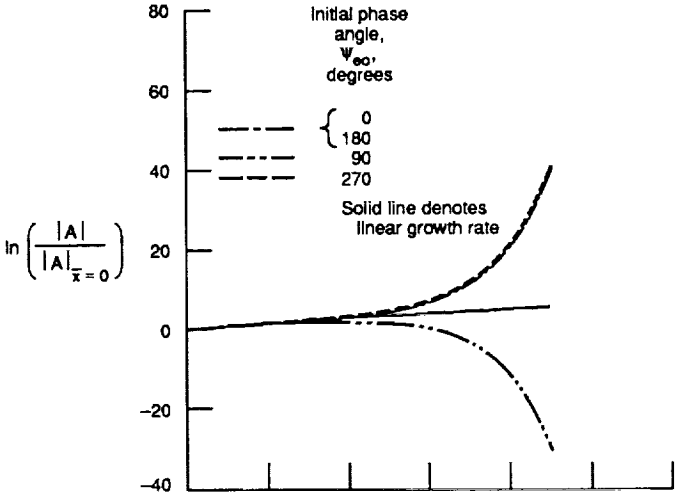

(a) Magnitude.

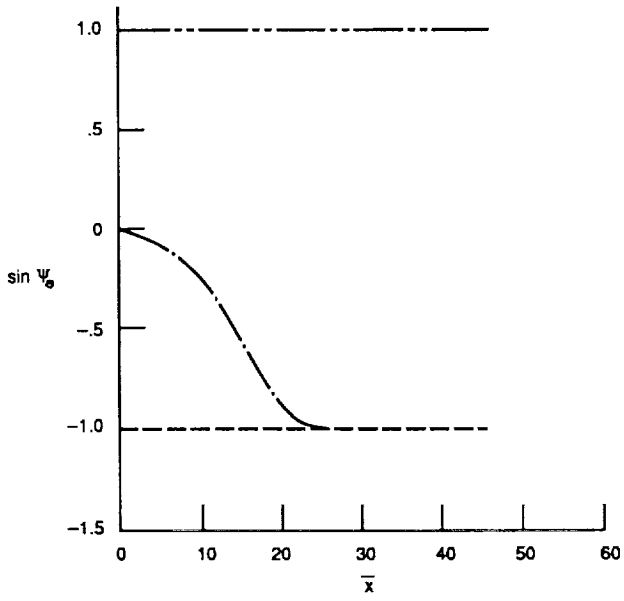

(b) Phase.

Figure 4.—Amplitude of the oblique waves in the nonlinear region. Amplitude of fundamental instability wave at $\bar{x} = 0$ $|a_o^o| = 1$; location of origin of disturbances $\bar{R}/\bar{R}_{up} = 0.8$; $\Psi_{eo} = 3\pi/2$.

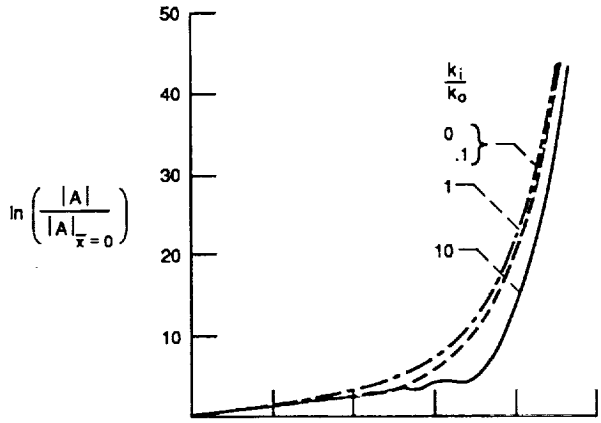

(a) Magnitude.

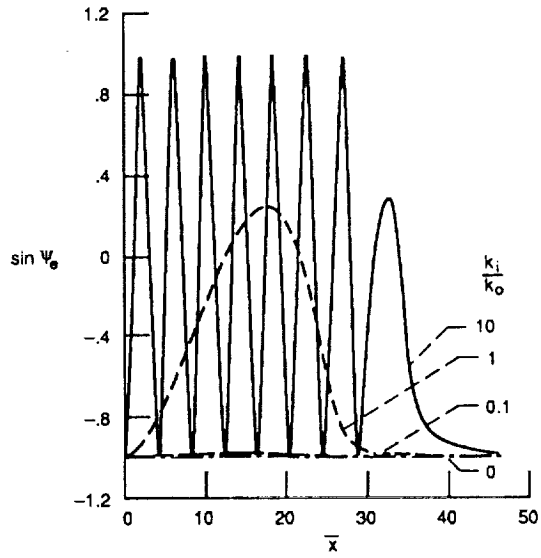

(b) Phase.

Figure 5.—Effect of detuning factor k_i on amplification of subharmonic; $\Psi_{eo} = 3\pi/2$; $|a_o^o| = 1.0$.

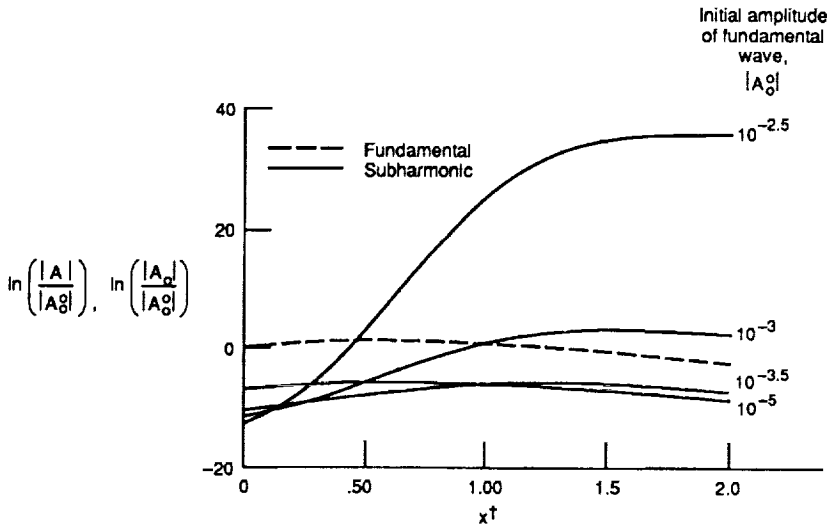

Figure 6.—Amplification curves for two-dimensional fundamental A_o and subharmonic oblique waves A at different initial amplitudes of fundamental wave $|A^o_{o,n}|$. Dimensionless frequency $F^* = 10^{-5}$; location of origin of disturbances $\bar{R}_i/\bar{R}_{up} = 0.8$; phase angle $\Psi_{oi} = 3\pi/2$; and subharmonic inital level, $A^o_n = 10^{-8}$.

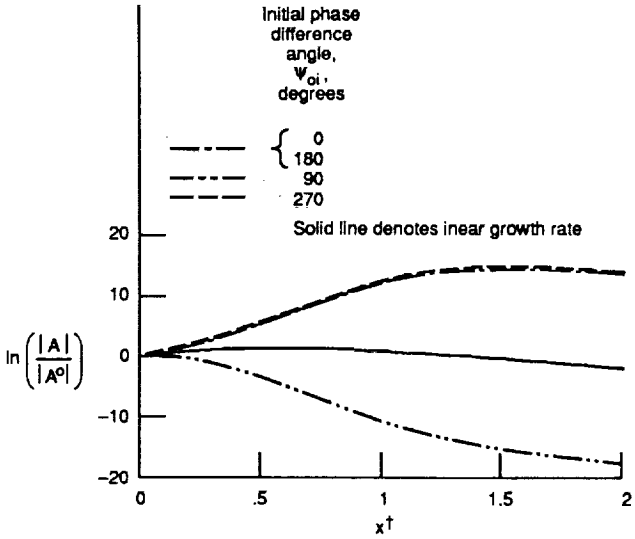

(a) Spatial variation of amplitude.

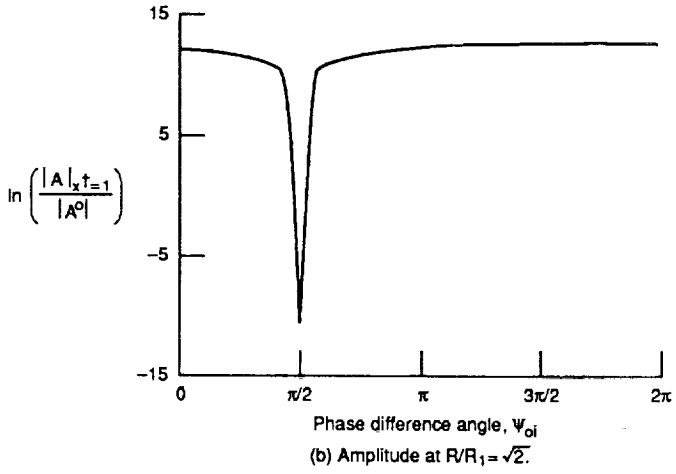

(b) Amplitude at $R/R_1 = \sqrt{2}$.

Figure 7.—Effect of initial phase-difference angle Ψ_{oi} on amplification of subharmonic. Dimensionless frequency $F^* = 10^{-5}$; location of origin of disturbances $\bar{R}_i/\bar{R}_{up} = 0.8$; initial amplitude of fundamental $|A^o_{o,n}| = 0.001$; and inital amplitude of subharmonic $A^o_n = 10^{-8}$.

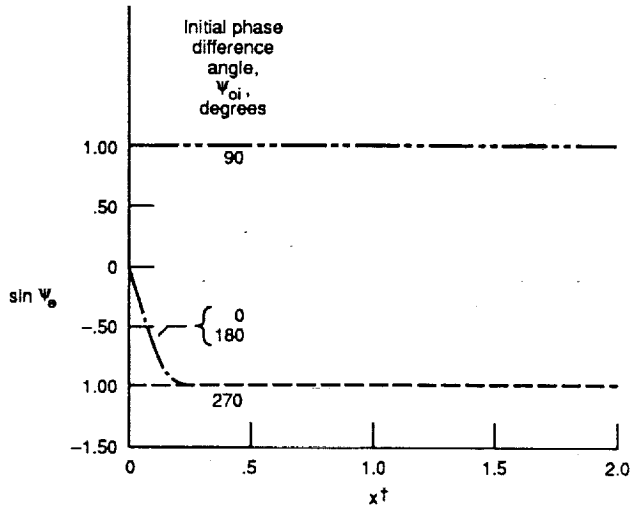

Figure 8.—Dependence of development of the phase angle Ψ_e on initial phase angle of fundamental Ψ_{oi}. Dimensionless frequency $F^* = 10^{-5}$; location of origin of disturbances $\bar{R}_i/\bar{R}_{up} = 0.8$; initial amplitude of fundamental $|A^o_{o,n}| = 0.001$; and initial amplitude of subharmonic $A^o_n = 10^{-8}$.

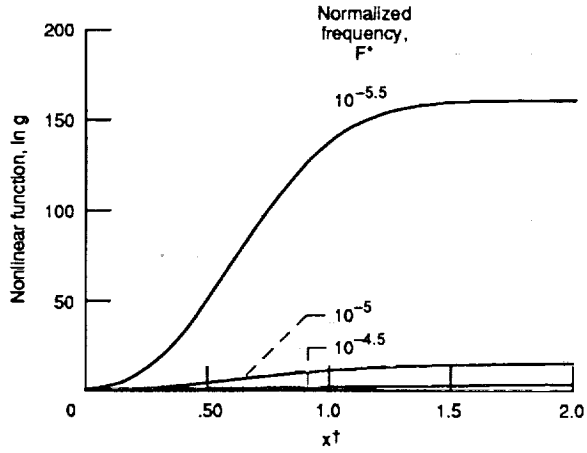

Figure 9.—Nonlinear amplification of subharmonic g for various values of dimensionless frequency F^*. Initial amplitude of fundamental $|A^o_{o,n}| = 0.001$; initial amplitude of subharmonic $A^o_n = 10^{-8}$; phase angle $\Psi_{oi} = 3\pi/2$; and location of origin of disturbances $\bar{R}_i/\bar{R}_{up} = 0.8$.

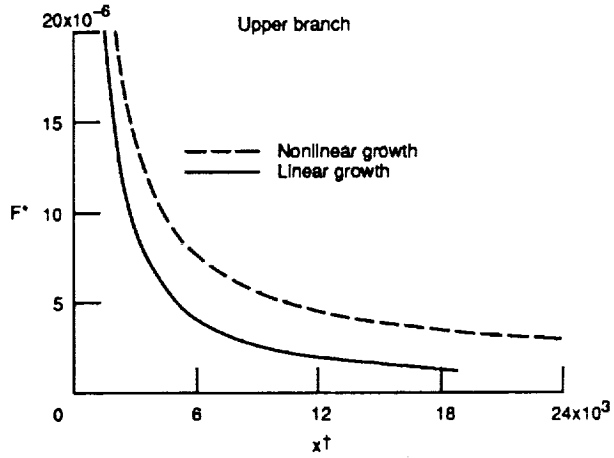

Figure 10.—Upper branches of neutral stability curves for nonlinear and linear development of oblique waves. Initial amplitude of fundamental $|A^{0}_{0,n}| = 0.001$; phase angle $\Psi_{oi} = 3\pi/2$; and location of origin of disturbances $\bar{R}_i/\bar{R}_{up} = 0.8$.

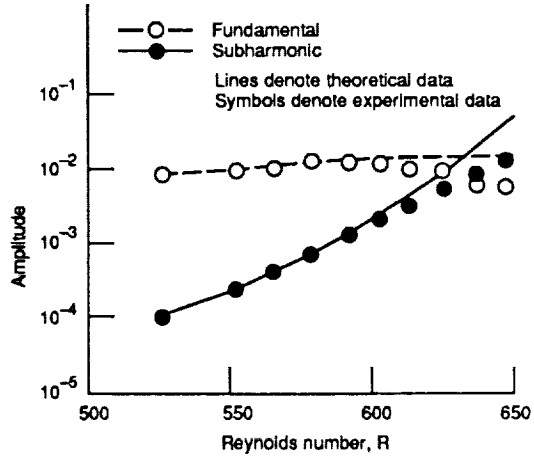

Figure 11.—Comparison of calculated amplitudes of fundamental and subharmonic streamwise velocities with experimental data of Kachanov and Levchenko (1984) at $F^* = 137 \times 10^{-6}$.

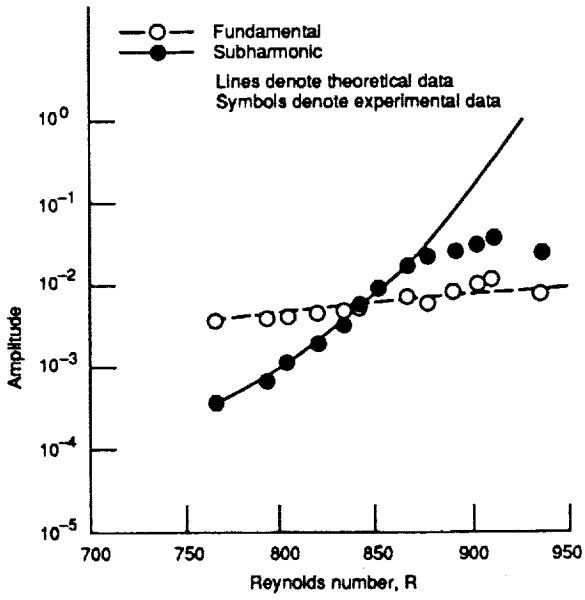

Figure 12.—Comparison of calculated amplitudes of fundamental and subharmonic streamwise velocities wth experimental data of Corke and Mangano (1987) at $F^* = 93 \times 10^{-6}$.

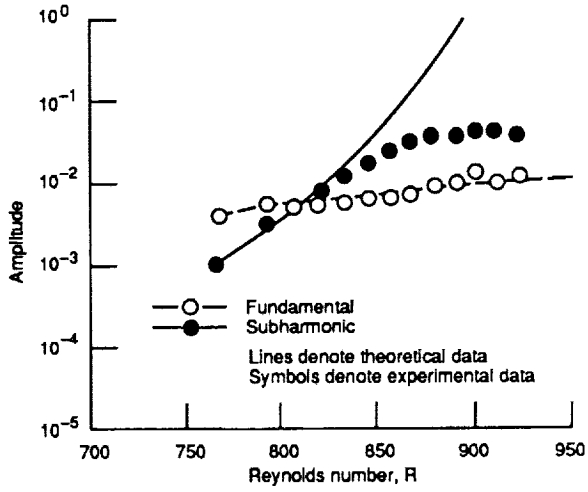

Figure 13.—Comparison of calculated amplitudes of fundamental and subharmonic streamwise velocities with experimental data of Corke and Mangano (1987) at $F^* = 82.7 \times 10^{-6}$.

NASA
National Aeronautics and Space Administration

Report Documentation Page

1. Report No.	2. Government Accession No.	3. Recipient's Catalog No.
NASA TM-103639		

4. Title and Subtitle	5. Report Date
Critical-Layer Nonlinearity in the Resonance Growth of Three-Dimensional Waves in Boundary Layers	November 1990
	6. Performing Organization Code

7. Author(s)	8. Performing Organization Report No.
Reda R. Mankbadi	E-5000
	10. Work Unit No.
	505-02-22

9. Performing Organization Name and Address	11. Contract or Grant No.
National Aeronautics and Space Administration Lewis Research Center Cleveland, Ohio 44135-3191	
	13. Type of Report and Period Covered
	Technical Memorandum

12. Sponsoring Agency Name and Address	14. Sponsoring Agency Code
National Aeronautics and Space Administration Washington, D.C. 20546-0001	

15. Supplementary Notes

16. Abstract

This paper addresses the nonlinear interactions of a triad of initially linear stability waves. The triad consisted of a single two-dimensional mode at a given frequency and two oblique modes with equal and opposite spanwise wave numbers. The oblique waves were at half the frequency and streamwise wave number of the two-dimensional mode. Attention was focused on the boundary-layer transition at low frequencies and high Reynolds numbers. A five-zoned structure and low-frequency scaling were used to derive the nonlinear-interaction equations. In this study, we analyzed the initial nonlinear development of the waves; the results indicated that the two-dimensional wave behaves according to linear theory. Nonlinear interactions caused exponential-of-an-exponential growth of the oblique modes. This resonant amplification of the subharmonic depended on the initial amplitude of the two-dimensional wave and on the initial phase angle between the two-dimensional wave and the oblique waves. The resonant growth of the oblique modes was more pronounced at lower frequencies than at higher frequencies. The results presented herein are in good agreement with experimental results and offer new explanations of the observed process.

17. Key Words (Suggested by Author(s))	18. Distribution Statement
Boundary layer Transition Nonlinear instability waves	Unclassified – Unlimited Subject Category 34

19. Security Classif. (of this report)	20. Security Classif. (of this page)	21. No. of pages	22. Price*
Unclassified	Unclassified	58	A04

NASA FORM 1626 OCT 86

*For sale by the National Technical Information Service, Springfield, Virginia 22161